A new macro-financial condition index for the euro area

Claudio Morana[*]

University of Milano-Bicocca, Center for European Studies (CefES), Rimini Centre for Economic Analysis (RCEA-Europe ETS; RCEA-HQ), Center for Research on Pensions and Welfare Policies (CeRP), 20126 Milano, Italy

ABSTRACT

A new time-domain decomposition for weakly stationary or trend stationary processes is introduced. The method is based on trigonometric polynomial modeling, and it is explicitly devised to disentangle medium to long-term and short-term fluctuations in macroeconomic and financial series. A multivariate extension involving sequential univariate decompositions and Principal Components Analysis is also provided. Based on this multivariate approach, new composite indexes of macro-financial conditions for the euro area are introduced. The indicators suggest that most of the GDP contraction during the current pandemic has been of short-term, cyclical nature. Moreover, the financial cycle might have currently achieved a peak area. Hence, the risk of further, deeper disruptions is high, particularly as a new sovereign/corporate debt crisis were not eventually avoided.

© 2021 EcoSta Econometrics and Statistics. Published by Elsevier B.V. All rights reserved.

1. Introduction

Since the burst of the early 2000s stock market bubble, and even more since the subprime financial crisis and its associated Great Recession, there has been a renewed interest in the literature for the understanding of financial crisis mechanics, their propagation across markets and institutions, their channels of transmission to the real economy, the cumulative feedback effects from the real to the financial sector, their anticipation through early warning indicator systems, and their measurement, monitoring, and forecasting. This is in light not only of the effect of vanishing asset values during financial bust episodes but also of the large macroeconomic displacements and long-lasting economic stagnations which financial crises might generate.

In this respect, the concept of the "financial cycle" appears to be fundamental to understand the ambivalent role of financial markets for economic growth. On the one hand, well-developed and smoothly operating financial markets are essential for economic prosperity, particularly in advanced economies, where the level of financial development is sufficiently high

---

* Corresponding author.
  E-mail address: claudio.morana@unimib.it

to operate on extensive margins, reaching large shares of the population. Financial development helps to correct frictions, like those related to information and transaction costs, improving the allocation of resources and saving and investment behavior, eventually fostering economic growth (Levine, 2005). On the other hand, beyond certain thresholds, financialization can become "excessive", turning into financial crises, eroding accumulated wealth, impairing intermediation activities and investment plans, and, eventually, damaging economic growth (Borio and Lowe, 2004).

Following Borio (2014), the financial cycle can be referred to as "the self-reinforcing interactions between perceptions of value and risk, risk-taking, and financing constraints". The typical development of a financial boom-bust episode is described through an accelerator mechanism, whereby rapid credit growth boosts property and asset prices, which in turn increase collateral values, and therefore the amount of credit that households and enterprises can obtain. This process continues until a threshold is overcome; thereafter it goes in reverse, eventually generating serious macroeconomic damages and economic stagnations (Jordà et al., 2013). During the building-up phase, excessive risk-taking behavior and balance sheets overstretching make the financial system increasingly fragile, therefore sowing the seeds of its destruction during the bust phase. The financial cycle peak tends to coincide with banking crises or periods of very high financial stress.

Measurement of the financial cycle, in relation to the prediction of its turning point and the associated recession risk, has therefore attracted growing interest in the literature. For instance, the predicting power of various proxy for the financial cycle, such as credit spreads, credit growth, balance sheet conditions, residential property prices, debt service ratio, has recently been investigated in Liu and Mönch (2016); Christiansen et al. (2019); Ponka (2017); Guender (2018); Borio and Drehmann (2019).

In this paper, we build on the above papers and propose a set of composite indicators of macro-financial conditions for the euro area. Relative to a pure financial cycle measure, our indicators are based on a broader information set, including also macroeconomic conditions. Given the strict interconnection between macroeconomic performance and financial market conditions, we aim to compute a composite measure of the macro-financial cycle, explicitly disentangling low and high-frequency macro-financial fluctuations (see also Kapetanios et al. (2018)).

In the light of the available empirical evidence (Borio and Drehmann, 2019), financial cycles appear to be concurrent with medium-term economic fluctuations, with a typical periodicity of fifteen to twenty years, lasting, therefore, longer than business cycle episodes, whose duration, historically, has not exceeded eight years in most countries. The causality between underlying macroeconomic and financial conditions runs in both directions, as medium-term financial fluctuations in asset prices can be expected to reflect fluctuations in macroeconomic fundamentals, i.e. revisions in expectations about their fundamentals; at the same time, financial markets developments impact the underlying macroeconomic context by affecting financial intermediation and credit flows, as well as agent expectations about overall economic conditions, and, therefore, their saving, consumption and investment decisions.

In our framework, these low-frequency developments in property and asset prices, as well as in macroeconomic variables, are denoted as medium to long-term or underlying macro-financial conditions. These are measured by macroeconomic and financial fluctuations of periodicity above ten years, consistent with the available evidence on the duration of the financial cycle (Borio and Drehmann (2019)), as well as with evidence showing that the duration of the business cycle might have recently increased (Beaudry et al. (2020)). On the other hand, macroeconomic and financial fluctuations of periodicity below ten years are denoted as short-term macro-financial conditions. These higher frequency fluctuations can be expected to reflect persistent interactions between the financial sector and the macroeconomy, occurring during business cycle episodes. Beaudry et al. (2020) have recently well characterized the type of forces behind the endogenous generation of the business cycle, pointing to strategic complementarities across agents and accumulation mechanisms of stock variables subject to threshold effects, whereby accumulation itself, beyond certain levels, tends to depress the individual value of accumulating more.

To disentangle medium to long-term and short-term macro-financial conditions, we introduce a new time-domain decomposition, based on trigonometric polynomial modelling of the underlying component of a stationary or trend stationary economic time series. The focus on stationary or trend stationary variables is justified by the fact that most of the economic variables which are informative for cyclical conditions such as financial returns, growth rates of macroeconomic variables, (some) imbalance measures, show these properties.

Intuitively, grounded on the Weierstrass Approximation Theorem, we aim to approximate the unknown function describing the medium to long-term evolution of an economic time series of interest using a parsimonious trigonometric polynomial specification. In this context, the empirical model is an approximation of the polynomial function, which in turn approximates the unknown function. The approximation provided by our empirical model exploits relevant economic information, improving upon purely statistical low-pass filters. Moreover, the procedure is set within a standard OLS regression framework and its implementation is straightforward. Monte Carlo evidence yields full support to the proposed methodology. We also introduce a multivariate extension for our decomposition, relying on a two-step approach, consisting of sequential application of the decomposition to the set of series of interest, and then the estimation of the common medium to long-term and short-term components through Principal Components Analysis.

Based on this multivariate approach, we introduce a set of new composite indexes of macro-financial conditions for the euro area. These indexes are devised in such a way to bear the interpretation of the expected overall, trend, and cyclical GDP growth. We then use our indicators to assess macro-financial conditions in the euro area over the last two decades. The sample is surely interesting, as it comprises the early 2000s stock market bubble burst, the 2007-2008 subprime financial crisis and ensuing Great Recession, the sovereign debt crisis and ensuing recession, and the pandemic crisis. The empirical

evidence shows that the proposed indicators yield valuable insights on all the crisis episodes. In particular, concerning the current pandemic recession, the indicators suggest that most of the contraction has been of short-term, cyclical nature. This is likely due to the prompt fiscal and monetary policy responses, which not only have sustained both the supply and demand sides of the euro area economy but have also avoided a major financial crisis. As shown by the Great Recession episode, major financial busts can generate long-lasting, sizable stagnations. In this respect, our evidence suggests that the financial cycle might have currently achieved a peak area. Hence, the risk for further, deeper disruptions is high, particularly in so far as a new sovereign/corporate debt crisis were not eventually avoided.

The paper is organized as follows. In Section 2 we introduce the new time-domain decomposition, its estimation, and multivariate extension. Still, in Section 2 we present the Monte Carlo results. In Section 3 we present the data. The results of the univariate and multivariate decompositions are presented in Section 4. In Section 5 we introduce three new composite indexes of macro-financial conditions and assess their information content for the euro area, with a special focus on the current pandemic recession. Finally, in Section 6 we conclude. In the Online Appendix, we report additional results concerning the Monte Carlo analysis and the estimation of the medium to long-term components for the euro area data assessed in this paper.

2. A new time-domain decomposition for economic time series

Since the seminal work of Beveridge and Nelson (1981) and Hodrick and Prescott (1997), various trend-cycle decompositions have been proposed for the case of I(1) processes, ranging from parametric to non-parametric models, from time to frequency domain methods, from time series model specifications to models based on theoretical assumptions on economic phenomena. For instance, in Beveridge and Nelson (1981) the trend component is computed as the optimal long-term forecast for an ARIMA process; on the other hand, in Hodrick and Prescott (1997) the definition of the trend is not grounded on the statistical knowledge of the DGP, but on the assumption that the trend component is determined by the process of economic growth, and therefore only vary smoothly over time. Alternative parametric decompositions to Beveridge and Nelson (1981) have also been proposed within the unobserved component framework (Nelson and Plosser, 1982; Harvey, 1985; Watson, 1986; Clark, 1987). In this framework, the time series models for the trend and cyclical components also show an ARIMA reduced form. For instance, in Harvey and Jaeger (1993) the trend is equivalent to an ARIMA(0,2,1) process, while the cycle to an ARMA(2,l) process. Differently, Baxter and King (1999) propose a frequency domain approach, where the trend component is computed from the low pass filter with cutoff set to yield fluctuations of periodicity larger than thirty-two quarters (eight years). Moreover, the cyclical component is computed as the difference between two low-pass filters with cutoffs set to yield cyclical fluctuations with periodicity between six and thirty-two quarters. More recently, Hamilton (2018) proposes an alternative to the Hodrick and Prescott (1997) filter, based on the definition of the cyclical component of a time series in terms of the h-period ahead forecast error for its linear projection on a constant and its four most recent values. The trend component is then obtained as the deviation of the actual series from its cyclical component.

In this paper, we introduce a parametric decomposition approach for weakly stationary series or trend stationary series. The decomposition aims to disentangle low and high-frequency fluctuations in economic time series, as they are related to different types of interactions involving macroeconomic and financial conditions.

Similar in spirit to Hodrick and Prescott (1997), we ground our decomposition on some empirical stylized facts and theoretical intuitions describing the financial cycle, rather than on the specification of its data generation process. We then denote as natural, or underlying, or medium-to long term component that component of an economic time series that is related to smooth swings in economic activity, the financial cycle, and their interaction. In the light of the findings in Borio and Drehmann (2019) and Beaudry et al. (2020), we associate to this component fluctuations of periodicity larger than ten years. Conversely, the short-term component reflects business cycle dynamics or even shorter-lived episodes. We associate the short-term component with fluctuations of periodicity smaller than ten years.

2.1. The MLT-ST decomposition

Given the weakly stationary or trend stationary processes $\{y_t\}$, $t = 1, .., T$, consider the following decomposition

$$y_t = n_t + a_t, \tag{1}$$

where $\{n_t\} \equiv \{g(\mathbf{v}_t^*)\}$ is the *natural* or *medium to long-term* (*MLT*) component and $\{a_t\}$ is the *short-term* (*ST*) component; $\{n_t\}$ and $\{a_t\}$ are orthogonal; $E_t[a_t] = E[a_t] = 0$, where E_t is the conditional expectation operator, given the available information on the underlying economic environment at time period t (I_t).

In the above decomposition (1), $g(\cdot)$ is the real valued function

$$g(\mathbf{v}_t^*) = \theta_0 + \theta_1 t + f(\mathbf{x}_t^*), \tag{2}$$

and $f(\mathbf{x}_t^*)$ is specified according to the following trigonometric expansion

$$f(\mathbf{x}_t^*) = \sum_{j=1}^{j^*} \theta_{s,j} \sin(2\pi j \frac{t}{T}) + \theta_{c,j} \cos(2\pi j \frac{t}{T}) +$$

$$\sum_{i=1}^{m}\sum_{j=1}^{j^*}\theta_{s,ij}\sin(2\pi j\frac{\sum_{k=1}^{t}x_{i,k}}{\sum_{k=1}^{T}x_{i,k}}) + \theta_{c,ij}\cos(2\pi j\frac{\sum_{k=1}^{t}x_{i,k}}{\sum_{k=1}^{T}x_{i,k}}), \tag{3}$$

where $\mathbf{v}_t^* = \begin{bmatrix} 1 & t & x_{1,t} & \cdots & x_{m,t} \end{bmatrix}'$ is a $(m+2)\times 1$ vector; the conditioning variables $x_{i,t}$, $i = 1,..,m$ are weakly stationary variables with $\sum_{k=1}^{T}x_{i,k}\neq 0$; θ_0, θ_1, $\theta_{s,j}$, $\theta_{c,j}$, $\theta_{s,ij}$, $\theta_{c,ij}$ are parameters; $I_t\equiv\mathbf{v}_t^*$. See Gallant (1981, 1984) for the seminal contribution on the Fourier flexible functional form; see also Baillie and Morana (2009, 2012); Becker et al. (2006); Lee and Enders (2012); Morana and Sbrana (2019), for recent applications.

In this context, the *MLT* component measures the underlying, smooth fluctuations of the series, with periodicity longer than business cycle episodes, i.e. longer than ten years (Borio and Drehmann, 2019; Beaudry et al., 2020), and bears the interpretation of conditional expectation for the series y_t, given information on the underlying economic environment ($I_t\equiv\mathbf{v}_t^*$). Hence, $n_t = E_t[y_t]$, where E_t is the conditional expectation operator. Moreover, the *ST* component is defined as the deviation of the actual series y_t from the *MLT* component, i.e. $a_t = y_t - n_t$. It shows fluctuations occurring with periodicity below ten years, including business cycle episodes and shorter-lived episodes. This disentangling is governed by the index j^*, as the angular velocity $\omega_j = \frac{2\pi j}{T}$ refers to a pair of sin and cosine waves which accomplish j cycles in the T periods spanned by the data, and therefore of periodicity $P = \frac{2\pi}{\omega_j} = T/j$.

2.2. Estimation of the MLT *and* ST *components*

The proposed decomposition can be easily implemented through OLS estimation of the following regression function

$$y_t = \theta_0 + \theta_1 t + \sum_{j=1}^{j^*}\theta_{s,j}\sin(2\pi j\frac{t}{T}) + \theta_{c,j}\cos(2\pi j\frac{t}{T}) +$$

$$\sum_{i=1}^{m}\sum_{j=1}^{j^*}\theta_{s,ij}\sin(2\pi j\frac{\sum_{k=1}^{t}x_{i,k}}{\sum_{k=1}^{T}x_{i,k}}) + \theta_{c,ij}\cos(2\pi j\frac{\sum_{k=1}^{t}x_{i,k}}{\sum_{k=1}^{T}x_{i,k}}) + \varepsilon_t, \tag{4}$$

where $t = 1,..,T$, ε_t is i.i.d. with zero mean, variance σ^2 and finite fourth moment, and the regressors $x_{i,t}$ $i = 1,...,m$ are weakly stationary processes. Under the above conditions, the model in (4) can be consistently estimated by OLS (Hamilton (1994); ch. 16), i.e.

$$\Upsilon_T\left(\hat{\theta} - \theta\right) \xrightarrow{d} N\left(\mathbf{0}, \sigma^2\mathbf{Q}^{-1}\right),$$

where $\theta = (\theta_0, \theta_1, \theta_{s,1}, .., \theta_{c,mj^*})$, $\mathbf{Q} = E[\mathbf{z}_t^{*\prime}\mathbf{z}_t^*]$, $\mathbf{z}_t^* = \left(1 \quad t \quad \sin(2\pi\frac{t}{T}) \quad ... \quad \sin(2\pi\frac{\sum_{k=1}^{t}x_{1,k}}{\sum_{k=1}^{T}x_{1,k}}) \quad ... \right)'$, and

$$\underset{(m+2)\times(m+2)}{\Upsilon_T} = \begin{bmatrix} \sqrt{T} & 0 & 0 & \ldots & 0 & 0 & 0 \\ 0 & T^{3/2} & 0 & \ldots & 0 & 0 & 0 \\ \vdots & \vdots & \sqrt{T} & \ldots & \vdots & \vdots & \vdots \\ 0 & 0 & 0 & \ldots & \sqrt{T} & 0 & 0 \\ 0 & 0 & 0 & \ldots & \ldots & \sqrt{T} & 0 \\ 0 & 0 & 0 & \ldots & 0 & 0 & \sqrt{T} \end{bmatrix}. \tag{5}$$

Notice in fact that, while the normalized partial sum of the weakly stationary series $x_{i,t}$, $i = 1,...,m$, i.e. $\frac{\sum_{k=1}^{t}x_{i,k}}{\sum_{k=1}^{T}x_{i,k}}$, is an integrated (I(1)) process, its periodic transformation behave asymptotically as stationary, zero-mean, homoskedastic AR(1) processes. This result, established in Granger and Hallman (1991) and Ermini and Granger (1993), appears to hold for periodic transformations of any I(1) process and not only for random walks (with or without drift). Supportive Monte Carlo evidence is provided in Dittmann and Granger (2002), where is shown that the estimated long-memory parameter of the sine and cosine of a random walk process has strong short-term correlations but not even long memory.

We then have

$$y_t = \hat{n}_t + \hat{a}_t, \tag{6}$$

where $\hat{n}_t \equiv \hat{y}_t$, i.e. the fitted component from the OLS regression in (4), and $\hat{a}_t \equiv \hat{\varepsilon}_t$, i.e. the estimated residual component. The algebra of OLS ensures that the two estimated components are orthogonal by construction.

Concerning the trigonometric expansion, a parsimonious specification can be easily determined by means of a general to specific reduction strategy, based on the statistical significance of the retained regressors, implemented through an autometrics/saturation algorithm (Hendry et al., 2008; Doornik, 2009; Castle et al., 2021), as available in the OxMetrics 8 package. As serial correlation and conditional heteroskedasticity can be expected in the estimated residuals $\hat{a}_t$, Newey-West autocorrelation and heteroskedastic consistent standard errors (HACSE) should be used for inference.

2.2.1. Insights on methodological underpinnings

Differently from purely statistical methods, the proposed decomposition directly exploits information on the underlying macroeconomic and financial context to extract the *MLT* and *ST* components from an economic time series of interest. Given the regression setting, the estimation of the *MLT* component depends on the selected specification, both in terms of conditioning variables $\mathbf{z}_t^*$ and the order of their trigonometric expansion j^*. While j^* is determined based on the periodicity of fluctuations to be shown by the *MLT* component (T/j^*), the actual specification of the $\mathbf{z}_t^*$ vector can be inspired by economic theory and the scope of the analysis itself. The application of a general to specific reduction strategy, through an autometrics/saturation algorithm, yields an effective way of selecting a most parsimonious final specification from an initial, potentially very large set of conditioning variables.

Hence, the proposed decomposition is data, theory, and scope driven, and inspired by the same theory of reduction used in dynamic econometrics (Hendry, 1995). The starting point of the analysis is the assumption that the data are generated from an unknown, high-dimensional probability distribution, i.e. the data generating process or DGP, which is characterized by a large set of parameters. The interest of the econometrician is then in some functions of these parameters, whose knowledge is required for testing theories, forecasting, policy simulation, and learning about the economy. Our decomposition surely fits within this last category of econometric modeling purposes.

Yet since the DGP itself can be expected to involve too many parameters to be estimated using the available data, reductions of the DGP are required. These reductions lead from the original DGP to the local DGP, which differently from the original DGP is described by the probability distribution of only a small subset of variables. Empirical modeling of this subset of variables yields an approximation of the local DGP, whose parameters can be estimated. Then, a parsimonious specification is eventually selected, through statical testing for the omission of relevant variables and misspecification tests.

However, our regression setting shows an important difference relative to the standard specification of an econometric model. In our context, grounded on (a special case of) the Weierstrass Approximation Theorem, whereby for every continuous function $f(\cdot)$ and every $\varepsilon > 0$, there exists a trigonometric polynomial $T(\cdot)$ such that $|f(z) - T(z)| < \varepsilon$ for all z, we aim to approximate the unknown function describing the medium to long-term evolution in an economic time series of interest using a parsimonious trigonometric polynomial specification. The empirical model is an approximation of the trigonometric polynomial, which in turn approximates the unknown function. The approximation provided by our empirical model is grounded on relevant economic information, which grants accuracy, informativeness, and interpretability to the estimated components.

We provide supportive Monte Carlo evidence on the effectiveness of the proposed methodology. In particular, we show that the proposed approach performs very satisfactorily in settings likely to hold in empirical applications with economic and financial data. We also show that the proposed approach overperforms a potential competitor, such as the boosted Hodrick-Prescott filter of Phillips and Shi (2020), albeit the advantage over the latter method is inversely proportional to the components' variance ratio.

2.3. Monte Carlo analysis

Consider the following DGP

$$y_t = n_t + a_t \tag{7}$$

for the weakly stationary or trend stationary series of interest $\{y_t\}$, $t = 1, .., T$, where $\{n_t\}$ is the *MLT* component, $\{a_t\}$ is the *ST* component, $\{n_t\}$ and $\{a_t\}$ are orthogonal, and $E_t[a_t] = E[a_t] = 0$.

In the simulation exercise, consistent with the empirical application, we consider two sample sizes $T = \{100, 300\}$, which are equivalent to 25 years of quarterly and monthly data, respectively. Accordingly, concerning the specification in (3), we set $j^* = 2$, to model fluctuations with periodicity above ten years. Moreover, we set $m = 1$.

The weakly stationary conditioning variable x_t is then specified according to the following zero mean, constant variance, AR(2) process

$$x_t = \phi_1 x_{t-1} + \phi_2 x_{t-2} + u_t,$$
$$u_t \sim i.i.d.N(0, 1), \tag{8}$$

with $0 < \phi_1 < 1$, $\phi_1 + \phi_2 < 1$, and $\phi_1 - \phi_2 = u[0.2, 0.8]$, where u is a uniform random variable over the range indicated; this allows for a very comprehensive range of serial correlation intensity in the *MLT* component.

For the *MLT* component n_t, the following four general models are then considered.

- M1:

$$n_t = \theta_{s,1} \sin(2\pi t/T) + \theta_{c,1} \cos(2\pi t/T) +$$
$$\theta_{c,2} \cos(4\pi t/T) + \theta_{s,21} \sin(2\pi \frac{\sum_{k=1}^{t} x_{i,k}}{\sum_{k=1}^{T} x_{i,k}}),$$

and $\theta_{s,1} = 1.7$, $\theta_{c,1} = -2.35$, $\theta_{c,2} = 0.7$, $\theta_{s,21} = -2.5$.

- M2:

$$n_t = \theta_{s,1} \sin(2\pi t/T) + \theta_{c,1} \cos(2\pi t/T)$$
$$+ \theta_{c,21} \cos(2\pi \frac{\sum_{k=1}^t x_{i,k}}{\sum_{k=1}^T x_{i,k}}) + \theta_{c,22} \cos(4\pi \frac{\sum_{k=1}^t x_{i,k}}{\sum_{k=1}^T x_{i,k}}),$$

and $\theta_{s,1} = 1.2$, $\theta_{c,1} = -1.5$, $\theta_{c,21} = 1.5$, $\theta_{c,22} = -0.5$.

- M3:

$$n_t = \theta_{c,1} \cos(2\pi t/T) + \theta_{s,21} \sin(2\pi \frac{\sum_{k=1}^t x_{i,k}}{\sum_{k=1}^T x_{i,k}}) +$$
$$\theta_{c,21} \cos(2\pi \frac{\sum_{k=1}^t x_{i,k}}{\sum_{k=1}^T x_{i,k}}) + \theta_{c,22} \cos(4\pi \frac{\sum_{k=1}^t x_{i,k}}{\sum_{k=1}^T x_{i,k}}),$$

and $\theta_{c,1} = -0.5$, $\theta_{s,21} = -0.1$, $\theta_{c,21} = -0.5$, $\theta_{c,22} = -0.05$.

- M4:

$$n_t = \theta_1 t + \theta_{s,1} \sin(2\pi t/T) + \theta_{s,22} \cos(4\pi \frac{\sum_{k=1}^t x_{i,k}}{\sum_{k=1}^T x_{i,k}}),$$

and $\theta_1 = -0.02$, $\theta_{s,1} = -0.5$, $\theta_{s,22} = 0.5$.

The above specifications are very general and differ in terms of the relative importance of the deterministic and stochastic components in the determination of the *MLT* component.

Finally, the *ST* component a_t is the zero mean weakly stationary AR(2) process

$$a_t = \varphi_1 a_{t-1} + \varphi_2 a_{t-2} + \nu_t,$$
$$\nu_t \sim i.i.d.N(0, \sigma_\nu^2),$$

with:

- $0 < \varphi_1 < 1$, $\varphi_1 + \varphi_2 < 1$, $\varphi_1 - \varphi_2 = u[0.2, 0.8]$, where u is a uniform random variable over the range indicated, in the general case of serially correlated *ST* component; this allows for a very comprehensive range of serial correlation intensity in the *ST* component.
- $\varphi_1 = \varphi_2 = 0$ in the special case of white noise *ST* component.

In both cases, σ_ν^2 is varied such that $(1 - R^2) \equiv \sigma_a^2/\sigma_y^2 = \{0.2, 0.3, 0.4, 0.5, 0.6, 0.7, 0.8\}$. Hence, in the exercise we also consider cases in which the variability of the *ST* component strongly dominates the variability of the *MLT* component. In fact, $\sigma_a^2/\sigma_n^2 = \frac{1}{R^2} - 1$, yielding $\sigma_a^2/\sigma_n^2 = \{0.25, 0.43, 0.67, 1, 1.5, 2.33, 4\}$.

The evaluation of the performance of the $MLT - ST$ decomposition is based on the Monte Carlo Theil's U statistic

$$U = \frac{\sqrt{\frac{1}{T} \sum_{t=1}^T (\hat{n}_t - n_t)^2}}{\sqrt{\frac{1}{T} \sum_{t=1}^T \hat{n}_t^2} + \sqrt{\frac{1}{T} \sum_{t=1}^T n_t^2}},$$

where n_t is the actual *MLT* component, generated according to DGPs M1-M4, and $\hat{n}_t$ its OLS estimate. By construction, U ranges between the optimal value of 0 ($\hat{n}_t$ and n_t are perfectly correlated) and the upper limit of 1 ($\hat{n}_t$ and n_t are uncorrelated). In all cases we consider 2000 Monte Carlo replications.

Apart from the correct specification case, we also assess the performance of a '" *feasible*" version of the proposed decomposition approach. In the feasible version we consider again DGPs M1-M4; yet rather than estimating the correctly specified model, we implement a general to specific model selection strategy, starting from the encompassing profligate model

$$y_t = \theta_0 + \theta_1 t + \sum_{j=1}^2 \theta_{s,j} \sin(2\pi j \frac{t}{T}) + \theta_{c,j} \cos(2\pi j \frac{t}{T})$$
$$+ \sum_{j=1}^2 \theta_{s,1j} \sin(2\pi j \frac{\sum_{k=1}^t x_{1,k}}{\sum_{k=1}^T x_{1,k}}) + \theta_{c,1j} \cos(2\pi j \frac{\sum_{k=1}^t x_{1,k}}{\sum_{k=1}^T x_{1,k}}) + \varepsilon_t, \tag{9}$$

where ε_t is the zero mean regression disturbance; $\theta_1 = 0$ in Models 1-3, and $\theta_1 \neq 0$ in M4. Model selection is then performed on the basis of the statistical significance of the retained regressors (1% significance level), using sequential t-ratio tests and Newey-West autocorrelation consistent standard errors for the estimated parameters.

For comparison, we also report Monte Carlo results for the boosted Hodrick-Prescott filter (*HP*; Phillips and Shi (2020)), which has been shown, both theoretically and in simulation experiments, to be able to recover trend components in a variety of frameworks, including deterministic drifts, structural breaks, in addition to integrated processes.
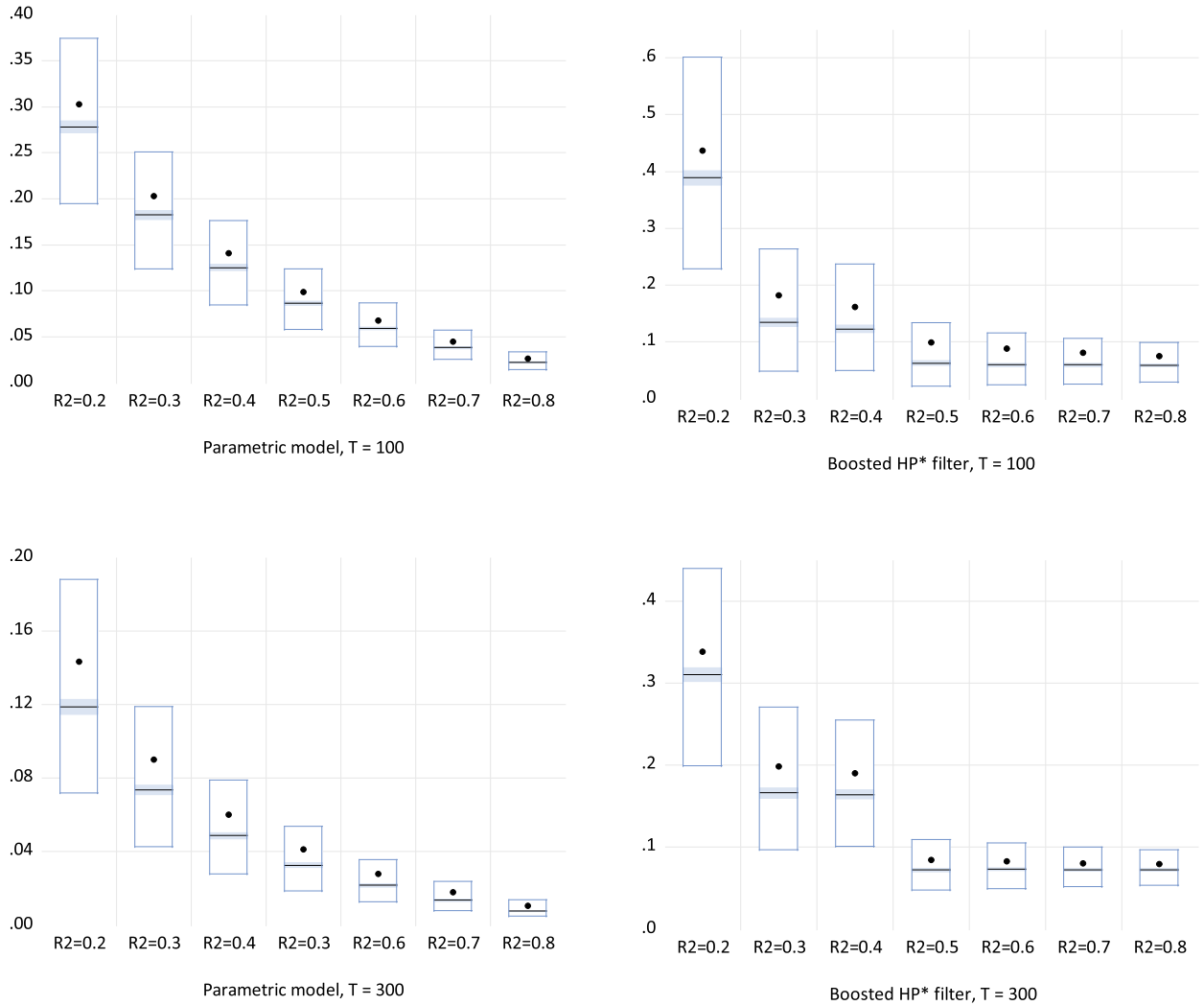
Fig. 1. Monte Carlo results, Theil's U index, Box Plots for Model 4 and autocorrelated cyclical component

We implement the boosted HP filter using an optimal value for the smoothing (penalization) parameter set according to the sample size. In this respect, we then follow Ravn and Uhlig (2002), who show that λ should vary by the fourth power of the frequency observation ratio. Then, for the case of $T = 100$, which is equivalent to 25 years of *quarterly* data, we set the smoothing (penalization) parameter λ equal to 1,600, i.e. the usual optimal value for this data frequency. We similarly do for the case of $T = 300$, which is equivalent to 25 years of *monthly* data, and therefore set λ equal to 129,600 (1600×3^4). Notice that DGPs M1-M4 imply that the investigated process is cyclical or trend-cyclical stationary. Once extracted the medium to long-term component, the residual series should then behave according to a weakly stationary process. Hence, in both cases, we use the KPSS test for level stationarity (5% level) as a backstop criterion. Moreover, we consider at most five iterations for the boosting algorithm.

We also implement an alternative version of the boosted HP filter (HP^*), allowing the smoothing parameter λ to change over the iterations of the boosting algorithm, still using the KPSS test for level stationarity (5% level) as backstop criterion. For instance, for the case of $T = 100$, we initially set λ equal to 1,600. Then, λ is kept unchanged for the first iteration of the boosting algorithm. It is successively switched to 129,600 (1600×3^4) for the following two iterations and set to 2,151,360 (1600×6^4) for the last two iterations. Moreover, for the case of $T = 300$, we initially set λ equal to 129,600 (1600×3^4) and keep it unchanged for the first iteration of the boosting algorithm; λ is successively switched to 2,151,360 (1600×6^4) in the following two iterations and set to 33,177,600 (1600×12^4) for the last two iterations.

2.3.1. Results

The results of the Monte Carlo exercise are reported in Table 1 Panels A-D and the box plots in Figures 1-2. In particular, without loss of generality, in Table 1 we report average figures for the Theil's U index and its standard deviation, computed across DGPs M1-M4. Detailed results for each model are reported in Tables A1-A12 in the Online Appendix.

Table 1

Monte Carlo results: Average results from Models 1-4, parametric decomposition and boosted HP filters

Panel A: autocorrelated cycle, T = 100							
σ_a^2/σ_n^2	4	2.33	1.5	1	0.67	0.43	0.25
U_p	0.173	0.110	0.074	0.050	0.034	0.023	0.013
σ_{U_p}	0.153	0.100	0.067	0.046	0.031	0.020	0.012
$U_{p,F}$	0.285	0.190	0.131	0.092	0.063	0.041	0.025
$\sigma_{U_{p,F}}$	0.159	0.113	0.080	0.056	0.039	0.026	0.015
U_{HP}	0.463	0.420	0.392	0.373	0.360	0.350	0.342
$\sigma_{U_{HP}}$	0.286	0.250	0.221	0.198	0.179	0.161	0.146
$U_{HP'}$	0.465	0.176	0.152	0.094	0.081	0.071	0.064
$\sigma_{U_{HP'}}$	0.288	0.193	0.164	0.131	0.112	0.092	0.077

Panel B: white noise cycle, T = 100							
σ_a^2/σ_n^2	4	2.33	1.5	1	0.67	0.43	0.25
U_p	0.073	0.043	0.028	0.019	0.012	0.009	0.005
σ_{U_p}	0.056	0.033	0.021	0.014	0.010	0.006	0.004
$U_{p,F}$	0.145	0.090	0.059	0.040	0.027	0.018	0.010
$\sigma_{U_{p,F}}$	0.070	0.044	0.029	0.020	0.013	0.009	0.005
U_{HP}	0.402	0.374	0.359	0.350	0.343	0.339	0.336
$\sigma_{U_{HP}}$	0.208	0.180	0.163	0.150	0.141	0.134	0.128
$U_{HP'}$	0.400	0.141	0.125	0.073	0.066	0.061	0.059
$\sigma_{U_{HP'}}$	0.208	0.133	0.115	0.088	0.075	0.067	0.063

Panel C: autocorrelated cycle, T = 300							
σ_a^2/σ_n^2	4	2.33	1.5	1	0.67	0.43	0.25
U_p	0.074	0.045	0.029	0.020	0.013	0.009	0.005
σ_{U_p}	0.078	0.048	0.031	0.021	0.014	0.009	0.006
$U_{p,F}$	0.135	0.084	0.056	0.038	0.026	0.017	0.010
$\sigma_{U_{p,F}}$	0.097	0.063	0.043	0.030	0.020	0.013	0.008
U_{HP}	0.382	0.359	0.346	0.338	0.332	0.328	0.325
$\sigma_{U_{HP}}$	0.213	0.184	0.164	0.150	0.140	0.131	0.125
$U_{HP'}$	0.381	0.184	0.169	0.080	0.076	0.072	0.069
$\sigma_{U_{HP'}}$	0.214	0.143	0.124	0.083	0.075	0.067	0.061

Panel D: white noise cycle, T = 300							
σ_a^2/σ_n^2	4	2.33	1.5	1	0.67	0.43	0.25
U_p	0.025	0.015	0.009	0.007	0.005	0.003	0.002
σ_{U_p}	0.018	0.011	0.007	0.005	0.003	0.002	0.001
$U_{p,F}$	0.052	0.031	0.020	0.014	0.009	0.006	0.003
$\sigma_{U_{p,F}}$	0.026	0.015	0.010	0.007	0.005	0.003	0.002
U_{HP}	0.348	0.337	0.331	0.328	0.326	0.324	0.323
$\sigma_{U_{HP}}$	0.154	0.139	0.131	0.125	0.121	0.118	0.116
$U_{HP'}$	0.347	0.160	0.153	0.071	0.069	0.068	0.067
$\sigma_{U_{HP'}}$	0.153	0.102	0.093	0.061	0.058	0.056	0.054

The table reports Monte Carlo results for the mean Theil's U statistics (U_i) and its standard deviation (σ_{U_i}) for the unfeasible (U_p, σ_{U_p}) and feasible ($U_{p,F}$, $\sigma_{U_{p,F}}$) parametric decompositions, the Phillips and Shi (2020) boosted Hodrick-Prescott filter (U_{HP}, $\sigma_{U_{HP}}$), and the modified-boosted HP filter ($U_{HP'}$, $\sigma_{U_{HP'}}$). The figures are averages of the results obtained from Model 1, Model 2, Model 3, and Model 4. In particular, Panels A and B refer to the case of autocorrelated and white noise short-term components, respectively, for a sample size T = 100 observations; Panels C and D refer to the case of autocorrelated and white noise short-term components, respectively, for a sample size T = 300 observations.

As shown in Table 1, independently of the filtering procedure, the performance of the proposed approach improves with the sample size, in terms of Theil's U index mean level and dispersion. Similarly, performance in terms of Theil's U mean and dispersion improves as the *ST* to *MLT* variance ratio σ_a^2/σ_n^2 decreases, as well as serial correlation in *ST* decreases. For instance, for the case of autocorrelated *ST* component (Panels A, C), our decomposition shows a Monte Carlo mean Theil's U statistic in the range 0.01-0.2 (0.005-0.074) for $T = 100$ ($T = 300$). The corresponding figures for the case of non serially correlated *ST* component (Panels B, D) are 0.005-0.073 (0.002-0.025). In all cases, the minimum value corresponds to the case where $\sigma_a^2/\sigma_n^2 = 1/4$, while the maximum is for $\sigma_a^2/\sigma_n^2 = 4$. Concerning the feasible version of the decomposition, Theil's U figures are in the range 0.03-0.29 (0.01-0.15) for $T = 100$ ($T = 300$) for the case of serially correlated *ST* component, and in the range 0.01-0.15 (0.003-0.05) for the case of non serially correlated *ST* component. Hence, also the *feasible* version of the decomposition performs very well, albeit slightly less well than for the case of correct specification, particularly when the variance ratio σ_a^2/σ_n^2 is very large. Still in this case, however, the proposed approach appears to be fully effective in disentangling the *MLT* and *ST* components.

Moreover, our decomposition always outperforms the boosted-HP filters, independently of sample size T, variance ratio σ_a^2/σ_n^2, and degree of serial correlation in *ST*. The modified boosted-*HP** filter outperforms the boosted-*HP* filter in all the
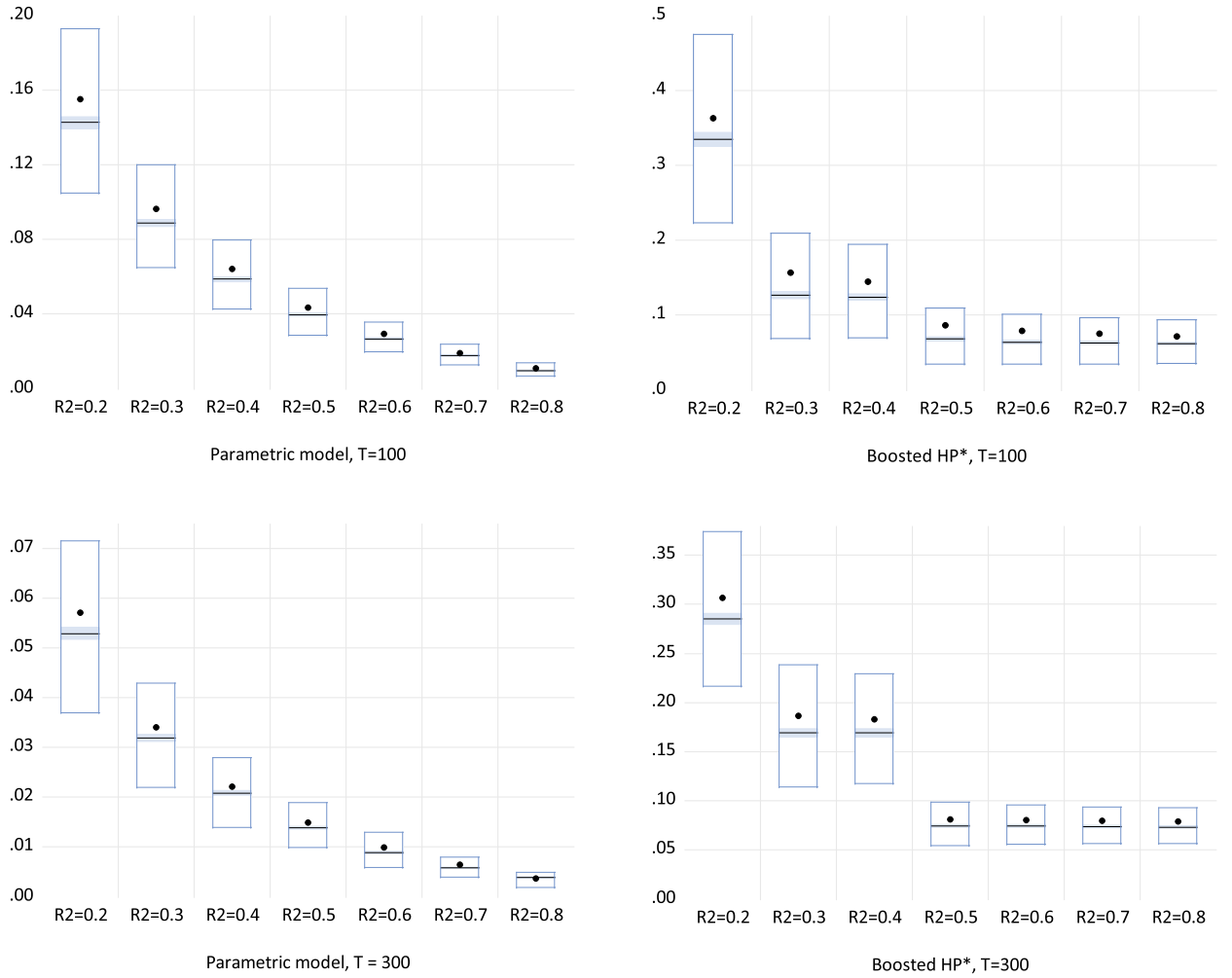
Fig. 2. Monte Carlo results, Theil's U index, Box Plots for Model 4 and white noise cyclical component

designs investigated, also showing a very satisfactory performance in most designs. Theil's U figures are in the range 0.06-0.47 (0.07-0.38) for $T = 100$ ($T = 300$) in the case of serially correlated ST component, and in the range 0.06-0.40 (0.05-0.15) in the case of non serially correlated ST component.

Similar conclusions concerning the relative ranking of the various approaches can be drawn by comparing the Monte Carlo standard deviations reported in Table 1. Clear-cut evidence can also be gauged from the inspection of Figures 1 and 2, where box plots are reported for the Theil's U index for Model 4 for illustrative purposes. Detailed results for all the DGPs are available in the Online Appendix.

2.4. The multivariate case

Following Morana (2007), consider the vector of N weakly stationary or trend stationary macroeconomic and financial variables of interest $\{\mathbf{y}_t\}$, characterized by common medium to long-term and short-term fluctuations. A multivariate version of the proposed $MLT - ST$ decomposition can then be written as

$$\mathbf{y}_t = \mathbf{n}_t + \mathbf{a}_t, \tag{10}$$

where $\mathbf{n}_t$ is the $(N \times 1)$ vector of medium to long-term components $n_{i,t}$, $i = 1, .., N$, and $\mathbf{a}_t$ is the $(N \times 1)$ vector of short-term components $a_{i,t}$, $i = 1, .., N$. The decomposition can then be implemented by means of a two-step procedure, based on sequential univariate $MLT - ST$ decompositions and Principal Components Analysis.

Hence, in the first step, the univariate decomposition in (1) is performed sequentially series by series; this yields

$$\mathbf{y}_t = \hat{\mathbf{n}}_t + \hat{\mathbf{a}}_t, \tag{11}$$

where the ($N \times 1$) vectors $\hat{\mathbf{n}}_t$ and $\hat{\mathbf{a}}_t$ contain the estimated *MLT* and *ST* components, respectively. Then, in the second step, the common medium to long-term and short-term components are estimated by Principal Components Analysis, applied to each set of estimated univariate components.

The decomposition can then be written as

$$\mathbf{y}_t = \hat{\boldsymbol{\Theta}}_{\mathbf{n}}\hat{\mathbf{f}}_{\mathbf{n},t} + \hat{\boldsymbol{\Theta}}_{\mathbf{a}}\hat{\mathbf{f}}_{\mathbf{a},t} + \hat{\mathbf{l}}_t, \tag{12}$$

where $\hat{\boldsymbol{\Theta}}_{\mathbf{n}} = \hat{\mathbf{Q}}_{\mathbf{n}}\hat{\mathbf{D}}_{\mathbf{n}}^{-1/2}$ is the estimated $N \times s$ common *MLT* factor loading matrix, $\hat{\mathbf{D}}_{\mathbf{n}} = diag\left\{\hat{\lambda}_{\mathbf{n}_1}, \hat{\lambda}_{\mathbf{n}_2}, ..., \hat{\lambda}_{\mathbf{n}_s}\right\}$ is the $s \times s$ diagonal matrix of the non-zero ordered eigenvalues of the sample variance-covariance matrix of the *MLT* processes $\hat{\boldsymbol{\Sigma}}_{\mathbf{n}}$ (rank $s < N$), $\hat{\mathbf{Q}}_{\mathbf{n}}$ is $N \times s$ matrix of the associated orthogonal eigenvectors, and $\hat{\mathbf{f}}_{\mathbf{n},t} = \hat{\mathbf{D}}_{\mathbf{n}}^{-1/2}\hat{\mathbf{Q}}_{\mathbf{n}}'\hat{\mathbf{n}}_t$ is the $s \times 1$ vector of the common *MLT* factors, as estimated by the s standardized principal components for the *MLT* series.

Similarly, $\hat{\boldsymbol{\Theta}}_{\mathbf{a}} = \hat{\mathbf{Q}}_{\mathbf{a}}\hat{\mathbf{D}}_{\mathbf{a}}^{-1/2}$ is the estimated $N \times r$ common *ST* factor loading matrix, $\hat{\mathbf{D}}_{\mathbf{a}} = diag\left\{\hat{\lambda}_{\mathbf{a}_1}, \hat{\lambda}_{\mathbf{a}_2}, ..., \hat{\lambda}_{\mathbf{a}_r}\right\}$ is the $r \times r$ diagonal matrix of the non-zero ordered eigenvalues of the sample variance-covariance matrix of the *ST* processes $\hat{\boldsymbol{\Sigma}}_{\mathbf{a}}$ (rank $r < N$), $\hat{\mathbf{Q}}_{\mathbf{a}}$ is $N \times r$ matrix of the associated orthogonal eigenvectors, and $\hat{\mathbf{f}}_{\mathbf{a},t} = \hat{\mathbf{D}}_{\mathbf{a}}^{-1/2}\hat{\mathbf{Q}}_{\mathbf{a}}'\hat{\mathbf{a}}_t$ is the $r \times 1$ vector of the common *ST* factors, as estimated by the r standardized principal components of the *ST* series.

Finally, $\hat{\mathbf{l}}_t = \left(\hat{\mathbf{n}}_t - \hat{\boldsymbol{\Theta}}_{\mathbf{n}}\hat{\mathbf{f}}_{\mathbf{n},t}\right) + \left(\hat{\mathbf{a}}_t - \hat{\boldsymbol{\Theta}}_{\mathbf{a}}\hat{\mathbf{f}}_{\mathbf{a},t}\right)$ is a $N \times 1$ vector of overall idiosyncratic components.

In terms of asymptotic properties, Bai (2003) establishes $min\left\{\sqrt{N}, \sqrt{T}\right\}$ consistency and asymptotic normality of $\hat{\mathbf{Q}}_{\mathbf{y}}'\mathbf{y}_t$, at each point in time, for the unobserved common components $\mathbf{Q}_{\mathbf{y}}\mathbf{y}_t$. Among other general conditions, this holds under the assumption of I(0) unobserved common factors and idiosyncratic components, where the latter might also display limited heteroskedasticity in both their time-series and cross-sectional dimensions. These results are extended to the case of I(1) un-observed common factors in Bai (2004). Since we rely on $\sqrt{T}$ consistent estimation of the $\mathbf{n}_t$ and $\mathbf{a}_t$ components, it appears that $\sqrt{T}$ ($T > N$) consistent estimation of the common components should also be granted in our framework. Supporting Monte Carlo evidence on the performance of PCA for the estimation of common components in a variety of frameworks, including those considered in this study, can be found in Morana (2007, 2014a).

Notice that the above procedure belongs to the general framework of the " Common Features " analysis originally proposed by Engle and Kozicki (1993). In our case, the common features shared by the N series are measured by the common *MLT* and *ST* components. Principal Components Analysis is then used to test for the presence of these common features, as well for their estimation. Notice that, by construction, the estimated idiosyncratic components, are free from the common features, i.e. "fail to have the feature(s) even though each of the series individually has the feature(s)", consistent with the definition proposed in Engle and Kozicki (1993).

3. The data

The data set covers a wide range of economic and financial variables for the euro area over the period 1999:1-2020:12. Full details are reported below.

Economic conditions and external and internal balance

Concerning **economic activity**, we use the **€-coin** series (ϵg), scaled to yield a monthly estimate of the year-on-year GDP growth rate. Concerning labor market conditions, we use the annual moving average of the monthly harmonized unemployment rate (u). Moreover, to assess the internal devaluation adjustment mechanism during economic downturns, we include the quarterly year-on-year rate of growth of **real earnings** (rw), while the monthly year-on-year **real effective exchange rate** return (ref) yields information on competitiveness and automatic adjustment through external demand. An increase in ref indicates real appreciation, i.e. a worsening in a country's terms of trade, anticipating a contraction in external demand and a worsening in the external balance. In this respect, external balance conditions are measured by the quarterly **current account balance** in the percentage of gross domestic product (caf). This series yields a measure of the net position of the euro area relative to the rest of the world, where a positive balance, i.e., *net lending* means that EA residents are net creditors/suppliers of funds to foreign residents; a negative balance, i.e., *net borrowing*, means the opposite. Internal balance is then measured by the quarterly public deficit to GDP ratio (dfg), computed using the annual moving sum of quarterly nominal gross domestic product. Monthly figures for caf and dfg are obtained from cubic interpolation of their quarterly figures, using actual series for end-points. The method followed assigns each value in quarterly series to the last monthly observation of the corresponding quarter. Then, it sets all intermediate monthly observations on a natural cubic spline connecting all the time points. See de Boor (1978) for details.

Prices, interest rates, and liquidity conditions

Concerning consumer prices, we consider the year-on-year monthly HCPI inflation rate (π). Moreover, concerning monetary conditions, we employ annualized real short- and long-term interest rates. In this respect, the **very short-term/policy real interest rate** is measured by the real *EONIA* overnight rate (oir), the **real short-term rate** is the 3-month real Euribor rate (sir), while the **real long-term interest rate** is the 10-year government bond rate (lir).

Additional measures of the monetary policy stance are also considered, such as the year-on-year monthly **real money growth rate** ($mr = m - \pi$), computed as the difference between the year-on-year monthly nominal M3 growth rate and

the year-on-year monthly HICP inflation rate; the **excess money growth rate** ($em = m-\epsilon g$), computed as the difference between the year-on-year monthly nominal M3 growth rate and the € -coin GDP growth rate.

Financial cyclical conditions

Financial cyclical conditions are monitored by various indicators. Firstly, we consider the quarterly **private credit gap**, i.e. the ratio of quarterly total credit to private nonfinancial sectors to the annual moving sum of quarterly nominal gross domestic product (Δcg). Moreover, we consider the quarterly **house price gap**, i.e. the ratio of the quarterly house price index to the annual moving sum of quarterly nominal gross domestic product (Δhg); the quarterly **house price to income ratio**, i.e. the quarterly nominal house price index divided by nominal net disposable income per head (Δhpi); the quarterly **house price to rent ratio**, i.e. the quarterly nominal house price index divided by the nominal rent price index (Δhpr). All the above-mentioned variables are (first) differenced for stationarity (year-on-year differences) and monthly figures are obtained from cubic interpolation of their quarterly figures, using actual series for end-points. Thirdly, we consider the year-on-year monthly **realgold price** return (gdr). Finally, concerning the stock market cycle, we consider the year-on-year monthly European Fama-French **market factor** return (mkt), i.e. the value-weight return of all (usable) firms, relative to the *risk-free* rate, measured by the three-month Treasury Bills rate (in monthly terms).

All the above variables have been found to provide insights on the self-reinforcing mechanism involving perceptions of value and risk, risk-taking, and financing constraints, which define boom-bust financial episodes (Borio, 2014). During a typical financial cycle, the rapid increase in credit to the private sector drives up property and asset prices, which in turn increase collateral values and thus the amount of credit the private sector can further obtain; this continues until misalignments between actual and natural/fundamental asset prices grow too large and balance sheets of financial institutions are overstretched, making them fragile and vulnerable. Then, the "bubble" bursts and misalignments are progressively corrected: as the process goes into reverse, a recession usually sets in, putting further stress on the financial system. In this respect, the financial cycle peak usually coincides with a phase of sizable financial stress or even a banking crisis.

Economic and financial uncertainty and financial condition measures

The set of financial stress indicators is comprised of interest rate spreads, uncertainty measures, and financial condition indexes. Among interest rate spreads, we consider the monthly **3-month Euribor-Eonia spread** ($soi = si - oi$), which yields an overall credit and liquidity risk measure for the interbank market; the monthly **term spread**, computed as the difference between the 10-year government bond rate and the 3-month Euribor rate ($lsi = li - si$). An increase in soi then points to rising interbank market stress; on the other hand, lsi appears to be related to business cycle fluctuations, being in general low at business-cycle peaks and high at business-cycle troughs. As a measure of **sovereign stress,** we consider the Composite Indicator of Systemic Sovereign Stress (SovCISS) by Garcia-de Andoain and Kremer (2018). SovCISS (sci) integrates measures of credit risk, volatility, and liquidity at short-term and long-term bond maturities into a broad measure of sovereign market stress. An increase in SovCISS points to increasing sovereign debt default risk. Moreover, the monthly VSTOXX implied volatility ($vstx$) is employed to measure economic and financial uncertainty (**stock market uncertainty**). An increase in the implied stock market volatility signals higher stock market uncertainty, which can be expected during an economic downturn. On the other hand, a decrease can be expected during an economic upturn (Schwert, 1989b; 1989a; Beltratti and Morana, 2006); see also Cipollini and Gallo (2019). Finally, we consider a monthly version of the new Composite indicator of systemic stress ($ciss$) introduced by Hollo et al. (2012). This composite indicator exploits information on bank and non-bank financial intermediaries, money markets, securities (equities and bonds) markets as well as foreign exchange markets. A monthly series is obtained by averaging daily figures over each month. An increase in this financial condition index points to increasing financial distress.

Expectations of future economic conditions

Concerning **expectations of future economic conditions**, we consider three **market-based measures of revisions in expectations** of future economic conditions, i.e. the year-on-year monthly European Fama and French (1993) **size** (smb) and **value** (hml) factors, and Carhart (1997) **momentum** (mom). The use of these risk factors is based on their property of mimicking state variables related to firms' economic and financial stress. For instance, consistent with the procyclical size and value effects, unanticipated higher profitability of small and value firms, i.e., positive *size* and *value* shocks might be related to favorable changes in the investment opportunity set and therefore to expectations of an improved macroeconomic outlook. Hence, positive size and momentum shocks might signal the expectation of an economic upturn. On the other hand, a positive momentum shock may not necessarily signal improved macroeconomic conditions. This is because *momentum* may persist not only over expansions but, temporarily, also over economic downturns. In fact, in the expectation of an incoming recession, *momentum* would be eroded progressively, as financial institutions lever down, shrinking stocks' liquidity. Yet if fundamentals are persistent and reflected in stock returns, firms with stronger fundamentals would outperform firms with weaker fundamentals also once the economic downturn sets in. Hence, positive momentum shocks might also reveal expectations of unfavorable changes in the investment opportunity set. In this respect, Morana (2017) documents a stable linkage between the conditional correlation for momentum and the € /US$ returns and the state of the business cycle for the euro area. The macroeconomic content of the Fama-French and Charart risk factors is assessed in Morana (2014b), where their connection to the state of the business cycle is also accounted in light of "news-driven" business cycle theory (Beaudry and Portier, 2014), whereby business cycle fluctuations are driven by abrupt changes in expectations. Coherently, Bagliano and Morana (2017) document that dynamic models augmented with lagged risk factor innovations could have predicted the timing and depth of the cyclical downturn and recovery associated with the Great Recession for the euro area, as well as the US and global economy, more accurately than standard forecasting models neglecting risk factors information.

4. Empirical results

Given the scope of the analysis, among the regressors used for the univariate decompositions, we only include the linear time trend (t) and the € -coin GDP growth rate ($x_{1,t} \equiv \text{€} \, g_t$; $m = 1$). Moreover, since the trigonometric specification is used to model medium to long-term fluctuations with periodicity larger than ten years, and given the time period covered in our empirical applications, i.e. about two decades of monthly data, the maximum order of the expansion we allow is $j^* = 2$. These specification choices then grants the association of the *MLT* components with low frequency GDP dynamics, coherent with their definition and objective of the decomposition. The residual, short-term component then accounts for the remaining higher frequency cyclical fluctuations.

Hence, the model in (4) can be written as

$$
y_t = \theta_0 + \theta_1 t + \sum_{j=1}^{2} \theta_{s,j} \sin(2\pi j \frac{t}{T}) + \theta_{c,j} \cos(2\pi j \frac{t}{T})
$$
$$
+ \sum_{j=1}^{2} \theta_{s,1j} \sin(2\pi j \frac{\sum_{k=1}^{t} x_{1,k}}{\sum_{k=1}^{T} x_{1,k}}) + \theta_{c,1j} \cos(2\pi j \frac{\sum_{k=1}^{t} x_{1,k}}{\sum_{k=1}^{T} x_{1,k}}) + \varepsilon_t. \tag{13}
$$

The above model is used for all the twenty-six series considered in the study, but the € -coin GDP growth rate. For the latter series, the regression model is specified as

$$
y_t = \theta_0 + \theta_1 t + \sum_{j=1}^{2} \theta_{s,j} \sin(2\pi j \frac{t}{T}) + \theta_{c,j} \cos(2\pi j \frac{t}{T}) + \varepsilon_t, \tag{14}
$$

as we (obviously) do not include its own contemporaneous trigonometric transforms in the set of conditioning regressors.

Starting from the above models, the final econometric specifications have then been obtained through a general to specific reduction strategy, grounded on the statistical significance of the retained regressors, using HACSE standard errors for inference. The final econometric models are reported in Table 2, Panels A-C.

As shown in the Table, the selected specifications are rather parsimonious, despite explaining a sizable proportion of the dependent variables in most cases. To assess the accuracy of the specification of the underlying component, in Table 2 we also report KPSS stationarity tests carried out on the estimated residuals (short-term components). In none of the cases, evidence of misspecification is detected, as the null hypothesis of level stationarity is never rejected at usual significance levels for any residual series.

In addition to the deterministic trigonometric components, various trigonometric transforms of the € -coin GDP growth rate have been retained in the specifications for all the series (apart from the € -coin, as already mentioned above). Their estimated medium to long-term components are then directly related to low-frequency fluctuations in GDP growth, confirming that relevant economic information is effectively exploited in the decompositions.

The estimated *MLT* components are reported in Figures B1-B3 in the Online Appendix. As shown in the plots, in all cases the decomposition appears to be successful in disentangling low-frequency fluctuations in the assessed series, therefore providing a valuable description of the underlying macro-financial context.

As detailed in the methodological Section, we then apply Principal Components Analysis (PCA) to the set of estimated *MLT* variables and the corresponding set of *ST* series (the estimated regression residuals), to subsume in few orthogonal indexes the information content of the data. The results are shown in Table 3, Panels A-B and Panels C-D, for the set of *MLT* and *ST* components, respectively. In particular, in the Table, we report the sample eigenvalues, which convey information on the proportion of total variance accounted by each principal component, and the sample eigenvector associated with the first principal component.

As shown in Table 3, Panel A, the first principal component $PC_{\hat{\mathbf{n}}_1, t} = \hat{\mathbf{Q}}'_{\hat{\mathbf{n}}_1} \hat{\mathbf{n}}_t$, alone accounts for about 30% of total variance for the *MLT* series; the second, third, and fourth components account for 16%, 15%, and 11% of the total variance, respectively. Moreover, the first principal component alone accounts for about 35% of the variance of the *MLT* component for GDP growth; the contributions of the second and third components are negligible, i.e. 1% and 4%, respectively; the contribution of the fourth component is more sizable, i.e. 19% (not reported); yet this latter component is likely to reflect idiosyncratic features, as it only accounts for 11% of total variance. As shown in Table 3, Panel C, similar conclusions can be drawn for the *ST* series as well. The first principal component $PC_{\hat{\mathbf{a}}_1, t} = \hat{\mathbf{Q}}'_{\hat{\mathbf{a}}_1} \hat{\mathbf{a}}_t$, accounts for about 30% of their total variance; the second, third, and fourth components account for 17%, 13%, and 7% of the total variance, respectively. Moreover, the first principal component alone accounts for about 50% of the variance of the *ST* component for GDP growth. Much smaller is the contribution of the second principal component, i.e. about 15%, while the contributions of the third and fourth factors are negligible, i.e. about 4% each (not reported). Given the scope of the analysis, we then focus our discussion on the interpretation of the first principal components $PC_{\hat{\mathbf{n}}_1}$ and $PC_{\hat{\mathbf{a}}_1}$ only. Hence, according to the notation used in the methodological section, we set $s = r = 1$.

Table 2
Stationarity tests and estimated decompositions

Panel A

	ϵg	Δu	rw	π	em	oir	sir	lir	smb
θ_0	4.123	-0.061	0.833	2.791	0.187	0.308	1.277	3.112	0.077
	(0.931)	(0.008)	(0.114)	(0.160)	(0.934)	(0.333)	(0.216)	(0.146)	(0.061
θ_1	0.023	3E-4	-	-0.003	0.030	-0.007	-0.010	-0.013	-
	(0.007)	(6E-5)	-	(0.001)	(0.007)	(0.002)	(0.002)	(0.001)	-
$\theta_{s,1}$	-1.432	-	- 0.539	-	- 4.348	1.334	0.999	-	-
	(0.563)	-	(0.204)	-	(0.303)	(0.221)	-	-	-
$\theta_{s,2}$	-1.265	0.036	-	-	-	-	-	0.372	-0.292
	(0,396)	(0.010)	-	-	-	-	-	(0.113)	(0.140)
$\theta_{c,1}$	0.928	-	-	-2.490	-	1.645	-	-	0.898
	(0.421)	-	-	(0.303)	-	(0.376)	-	-	(0.132)
$\theta_{c,2}$	-	0.072	-	-0.847	-	0.348	-	0.286	-
	-	(0.012)	-	(0.240)	-	(0.131)	-	(0.125)	-
$\theta_{s,1,1}$	-	-0.055	-	2.326	-	-0.987	-	-0.309	-
	-	(0.010)	-	(0.338)	-	(0.358)	-	(0.151)	-
$\theta_{s,1,2}$	-	-	0.254	-	-1.466	-	-	-	0.481
	-	-	(0.140)	-	(0.447)	-	-	-	(0.089)
$\theta_{c,1,1}$	-	-0.094	-	1.295	-	-	0.895	-	-0.377
	-	(0.013)	-	(0.280)	-	-	(0.140)	-	(0.120)
$\theta_{c,1,2}$	-	0.046	-0.278	-	-	-0.975	-0.723	-0.314	-0.928
	-	(0.007)	(0.131)	-	-	(0.176)	(0.130)	(0.096)	(0.145)
R^2	0.282	0.721	0.119	0.567	0.350	0.729	0.719	0.802	0.539
$\bar{R}^2$	0.271	0.715	0.108	0.559	0.343	0.723	0.715	0.798	0.536
$KPSS$	0.342	0.195	0.116	0.103	0.136	0.099	0.073	0.195	0.090
$KPSS_c$	0.033	0.028	0.051	0.040	0.040	0.062	0.091	0.031	0.084

Panel B

	hml	mom	ref	caf	lsi	fdg	Δhg	Δhpi	Δhpr
θ_0	1.669	-0.212	-2.578	-1.142	2.527	-0.203	-4.677	-1.674	-0.646
	(0.408)	(0.422)	(1.184)	(0.120)	(0.307)	(0.390)	(1.296)	(0.338)	(0.298)
θ_1	-0.011	0.007	0.021	0.012	-0.006	-0.010	0.041	0.014	0.015
	(0.003)	(0.003)	(0.008)	(9E-4)	(0.002)	(0.002)	(0.011)	(0.002)	(0.002)
$\theta_{s,1}$	-1.986	2.087		-	-1.962	-0.803	4.895	3.669	4.948
	(0.448)	(0.600)			(0.189)	(0.373)	(0.871)	(0.227)	(0.407)
$\theta_{s,2}$	-1.305	1.526	-	0.342	-	-1.420	2.346	-	-
	(0.307)	(0.413)		(0.123)		(0.255)		(0.525)	
$\theta_{c,1}$	1.146	-	-3.754	1.326	-0.456	-1.538	-	3.115	2.181
	(0.247)		(0.531)	(0.160)	(0.205)	(0.420)		(0.312)	(0.287)
$\theta_{c,2}$	-3.175	-1.462	-	-0.775	0.742	-1.945	-	-0.489	-2.424
	(0.619)	(0.534)		(0.077)	(0.106)	(0.359)		(0.177)	(0.448)
$\theta_{s,1,1}$	-	-	-	-1.094	-	3.147	-	-2.280	-
				(0.180)		(0.516)		(0.346)	
$\theta_{s,1,2}$	-0.628	0.630	-3.528	-	-	0.333	-	-	-
	(0.210)	(0.229)	(0.705)			(0.159)			
$\theta_{c,1,1}$	-3.175	2.992	-	-	-1.628	2.445	-	-	2.809
	(0.619)	(0.770)			(0.235)	(0.499)			(0.502)
$\theta_{c,1,2}$	-	-1.158	3.798	0.312	0.843	-0.641	-	-	-1.005
		(0.276)	(0.760)	(0.113)	(0.155)	(0.170)			(0.234)
R^2	0.563	0.311	0.404	0.886	0.691	0.842	0.583	0.797	0.806
$\bar{R}^2$	0.551	0.292	0.395	0.884	0.684	0.836	0.579	0.793	0.802
$KPSS$	0.536	0.071	0.114	0.230	0.185	0.223	0.295	0.348	0.407
$KPSS_c$	0.030	0.026	0.079	0.027	0.037	0.034	0.033	0.036	0.033

Panel C

	gdr	mkt	mr	Δcg	$vstx$	$ciss$	soi	sci
θ_0	-11.374	0.423	-1.195	2.329	23.871	0.161	0.353	0.210
	(3.495)	(0.159)	(0.702)	(0.345)	(0.880)	(0.015)	(0.042)	(0.013)
θ_1	0.125	-	-	-	-	-	-7E-4	-
	(0.025)						(3E-4)	
$\theta_{s,1}$	16.118	-	6.104	3.574	-	-	-	-0.065
	(3.994)		(0.564)	(0.617)				(0.020)
$\theta_{s,2}$	-	-	-	-	4.342	-	-	-0.055
					(1.241)			(0.019)
$\theta_{c,1}$	-	-	5.654	-	-	-0.081	-0.456	-0.083
			(0.970)			(0.028)	(0.044)	(0.025)
$\theta_{c,2}$	7.898	-0.525	-	-	4.101	0.146	-	-0.305
	(1.706)	(0.234)			(1.264)	(0.024)		(0.025)

Table 2 (*continued*)

Panel C

	gdr	mkt	mr	$\triangle cg$	vstx	ciss	soi	sci
$\theta_{s,1,1}$	-	-	-4.666	-	-	-	0.230	0.154
			(0.808)				(0.043)	(0.029)
$\theta_{s,1,2}$	-	1.182	-0.898	0.674	-	-0.072	-	-0.022
		(0.227)	(0.389)	(0.341)		(0.021)		(0.009)
$\theta_{c,1,1}$	-	-	-	1.445	-	-	0.279	0.124
				(0.652)			(0.033)	(0.016)
$\theta_{c,1,2}$	-8.326	-	-1.629	-1.474	-4.552	-0.046	-0.043	0.038
	(1.967)		(0.475)	(0.553)	(1.340)	(0.017)	(0.021)	(0.011)
R^2	0.396	0.302	0.610	0.369	0.291	0.501	0.725	0.798
$\bar{R}^2$	0.387	0.297	0.601	0.354	0.283	0.493	0.729	0.793
KPSS	0.108	0.099	0.249	0.556	0.327	0.182	0.328	0.367
$KPSS_c$	0.035	0.056	0.047	0.063	0.159	0.044	0.021	0.044

The table, Panels A-C, reports the estimated econometric models employed for the decomposition of the various variables. HACSE standard errors are reported in square brackets. R^2 and $\bar{R}^2$ are the unadjusted and adjusted coefficients of determination. KPSS (KPSSc) is the Kwiatkowski, Phillips, Schmidt and Shin test for stationarity or trend stationarity conducted on the actual variables (estimated residuals). The asymptotic critical values for the null hypothesis of stationarity (trend stationarity) are 0.739, 0.463, and 0.347 (0.216, 0.146, and 0.119) for the 1%, 5% and 10% level, respectively. The series are the monthly GDP growth rate ($\in g$), the change in the monthly unemployment rate ($\triangle u$), the quarterly real wage growth rate (rw), the monthly inflation rate (π), the monthly excess money growth rate (em), the monthly real overnight, short- and long-term interest rates (oir, sir, lir), the monthly Fama-French size, value and market factors ($smb, value, mkt$), the Charart momentum factor (mom), the monthly real effective exchange rate return (ref), the monthly interpolated current account to GDP ratio (caf), the monthly interpolated fiscal deficit to GDP ratio (fdg), the monthly term spread (lsi), the year-onyear change in the monthly interpolated house price to GDP ratio ($\triangle hg$), house price to income ratio ($\triangle hpi$), and house price to rent ratio ($\triangle hpr$), the monthly real gold price return (gdr) and real M3 growth rate (mr), the year-on-year change in the monthly interpolated credit to GDP ratio ($\triangle cg$), the monthly Stoxx implied volatility index ($vstx$), the monthly composite financial condition index ($ciss$), the monthly Euribor-Eonia spread (soi), and the monthly composite indicator of systemic sovereign stress (sci).

4.1. The common MLT and ST components

As shown by the estimated loadings in Table 3, Panel B, $PC_{\hat{\mathbf{n}}_1}$ exhaustively subsumes information about the underlying macro-financial environment. In particular, an increase in $PC_{\hat{\mathbf{n}}_1}$ can be associated with an improvement in underlying macro-financial conditions.

In fact, $PC_{\hat{\mathbf{n}}_1^*}$ loads with *positive* weight the *MLT* components, or their change ($\triangle$), for GDP growth ($\hat{n}_{\in g}$), real wages growth ($\hat{n}_{rw}$), real overnight ($\triangle\hat{n}_{oir}$) and short-term ($\triangle\hat{n}_{sir}$) rates, excess money growth ($\triangle\hat{n}_{em}$) and inflation ($\triangle\hat{n}_\pi$) rates; size ($\hat{n}_{smb}$), value ($\hat{n}_{hml}$), momentum ($\hat{n}_{mom}$), and market ($\hat{n}_{mkt}$) factor returns; real effective exchange rate returns ($\hat{n}_{ref}$), the current account to GDP ratio ($\hat{n}_{caf}$), the fiscal deficit to GDP ratio ($\hat{n}_{\triangle fg}$), the credit gap ($\hat{n}_{\triangle cg}$), the house price gap ($\hat{n}_{\triangle hg}$), the house price to income ratio ($\hat{n}_{\triangle hg}$), the house price to rent ratio ($\hat{n}_{\triangle hpr}$), and real M3 growth ($\hat{n}_{mr}$).

Moreover, $PC_{\hat{\mathbf{n}}_1}$ loads with *negative* weight the *MLT* components for the unemployment rate ($\hat{n}_{\triangle u}$), real gold price returns ($\hat{n}_{gdr}$), the implied volatility for the Stoxx index ($\hat{n}_{vstx}$), the Euribor-Eonia spread ($\hat{n}_{soi}$), the composite indicator of systemic sovereign stress ($\hat{n}_{sci}$), and the composite financial condition index ($\hat{n}_{ciss}$). $PC_{\hat{\mathbf{n}}_1}$ also loads with negative weight the term spread ($\hat{n}_{lsi}$) and the long-term real interest rate ($\triangle\hat{n}_{lir}$).

Hence, a typical improvement in the *underlying/medium to long-term* macro-financial environment in the euro area would be characterized by an increase in GDP growth and real wages and a contraction in unemployment. This pattern is consistent with an increase in productivity inducing an upward shift in labor demand and reducing the natural rate of unemployment. An improvement in underlying macro-financial conditions would also be characterized by growing inflation and expanding liquidity and credit; a rising real short-term interest rate and a real appreciation of the effective exchange rate; an improvement in the external (current account) and domestic (public deficit) balances. On the other hand, the long-term rate, and therefore the term spread, would contract. The improved economic outlook would also be characterized by positive size, value and momentum factor returns. This outlook is consistent with the overperformance of small and value stocks in an environment of improving economic conditions, as well as with the overperformance of firms with strong fundamentals. In this context, also overall financial conditions would tend to improve, as reflected in stable interbank and sovereign bond markets, expanding house and stock market prices, and falling economic uncertainty (implied stock market volatility). Falling gold price returns in a typical economic upturn might finally indicate that the underlying euro area macro-financial context is synchronous with global developments, consistent with three out of four of the major episodes of financial stress in our sample being global.

According to the above evidence, the building up of the financial cycle occurs during periods of sustained economic growth and rising asset (stock and house) prices, expanding credit and liquidity, improving domestic and foreign imbalances,

Table 3

Principal components analysis and macro-financial condition index estimation

Panel A: Selected estimated eigenvalues, medium to long-term components								
	PC_1	PC_2	PC_3	PC_4	PC_5	PC_6	PC_7	PC_8	PC_9
Eigen	7.744	4.089	3.834	2.810	2.184	1.645	1.198	0.948	0.600
% var	29.79	15.73	14.75	10.81	8.40	6.33	4.61	3.65	2.31
% cum	29.79	45.51	60.26	71.07	79.47	85.80	90.40	94.05	96.36

Panel B: Selected estimated eigenvector: loadings on PC_1, medium to long-term components								
	$n_{\epsilon g}$	$n_{\Delta u}$	$n_{\Delta rw}$	$n_{\Delta \pi}$	$n_{\Delta em}$	$n_{\Delta oir}$	$n_{\Delta sir}$	$n_{\Delta lir}$	$n_{\Delta smb}$
loading	0.208	-0.256	0.175	0.045	0.180	0.051	0.127	-0.026	0.074
	n_{hml}	n_{mom}	n_{ref}	n_{caf}	n_{lsi}	n_{fdg}	$n_{\Delta hg}$	$n_{\Delta hpi}$	$n_{\Delta hpr}$
loading	0.048	0.028	0.145	0.137	-0.243	0.263	0.253	0.306	0.324
	n_{gdr}	n_{mkt}	n_{mr}	$n_{\Delta cg}$	n_{vstx}	n_{ciss}	n_{soi}	n_{sci}	
loading	-0.226	0.055	0.210	0.075	-0.226	-0.293	-0.290	-0.303	

Panel C: Selected estimated eigenvalues, short-term components								
	PC_1	PC_2	PC_3	PC_4	PC_5	PC_6	PC_7	PC_8	PC_9
eigen	7.520	4.353	3.374	1.911	1.397	1.213	0.951	0.779	0.695
% var	28.92	16.74	12.98	7.35	5.37	4.66	3.66	3.00	2.67
% cum	28.92	45.66	58.64	65.99	71.36	76.03	79.68	82.68	85.35

Panel D: Selected estimated eigenvector: loadings on PC_1, short-term components loading								
	$a_{\epsilon g}$	$a_{\Delta u}$	a_{rw}	a_{π}	a_{em}	a_{oir}	a_{sir}	a_{lir}	a_{smb}
loading	0.261	-0.242	-0.300	0.219	-0.285	-0.235	-0.237	-0.169	0.030
	a_{hmt}	a_{mom}	a_{ref}	a_{caf}	a_{lsi}	a_{fdg}	$a_{\Delta hg}$	$a_{\Delta hpi}$	$a_{\Delta hpr}$
loading	0.026	-0.063	-0.082	0.020	0.142	-0.146	-0.153	0.240	0.314
	a_{gdr}	a_{mkt}	a_{mr}	$a_{\Delta cg}$	a_{vstx}	a_{ciss}	a_{soi}	a_{sci}	
loading	0.083	0.253	-0.278	-0.177	-0.201	-0.193	-0.091	-0.122	

Panel E: Estimation of the macro-financial condition index					
ϵg	$\mu_{\epsilon g}$	$\beta_{PC1.t}$	$\beta_{PC1.c}$	R^2	$\bar{\bar{R}}^2$
Coeff	1.058	0.328	0.463	0.539	0.536
	(0.186)	(0.068)	(0.084)		
$R^2 biv$		0.197	0.363		

In the table, Panels A-E report the results for Principal Component Analysis. In particular, in Panel A (C) we report the estimated selected eigenvalues (eigen) corresponding to the largest nine principal components ($PC_1, ...PC_9$) of the estimated medium to long-term (short-term) components, their percentage of accounted total variance (% var), and the cumulative percentage of accounted variance (% cum). In Panel B (D) we report the estimated loadings for the selected first principal component PC_1 for the various medium to long-term (short-term) components. Finally, in Panel E we report the estimated regression of the actual annualized monthly rate of €-coin GDP growth (€g) on a constant and the first principal components extracted from the standardized medium to long-term ($PC_{1,n}$) and short-term ($PC_{1,a}$) components, whose fitted values yields the composite index for overall macro-financial condition MF (eq. 17 in the main text). In panel E we also report the unadjusted and adjusted coefficients of determination (R^2 and $\bar{R}^2$), while $R^2 biv$ denotes the unadjusted coefficient of determination in the bivariate regression of € g on each of the first principal components ($PC_{1,n}$ and $PC_{1,a}$), whose fitted values yields the composite indexes for trend (MFt) and cyclical (MFc) macro-financial conditions, as defined in eq. 15 and eq. 16, respectively, in the main text.

and falling real long-term interest rates. In this context, economic and financial expansions are aligned and fuel each other. Moreover, a falling real long-term interest rate is consistent with saving glut-type conditions, where excess savings (over real investment) keep low real long-term interest rates, despite the central bank raises the policy rate and the real short-term interest rates. Hence, as a consequence, the term spread would also contract. This pattern is consistent with the evidence available for the euro area, as well as for other industrialized countries, over the period investigated. See also Bernanke (2005).

Symmetrically, a typical worsening in the underlying macro-financial environment would be characterized by opposite dynamics to those described above. Economic and financial contractions would also be aligned and fuel each other during the downward phase of the financial cycle.

Similarly, valuable information is provided by the estimated loadings for $PC_{\hat{a}_1}$ (Table 3, Panel D). In particular, an increase in $PC_{\hat{a}_1}$ can be associated with an improvement in short-term, cyclical macro-financial conditions. In this respect, $PC_{\hat{a}_1}$ loads with positive weight the ST components for GDP growth ($\hat{a}_{\epsilon g}$) and inflation ($\hat{a}_{\pi}$). It also loads positively on the size ($\hat{a}_{smb}$), value ($\hat{a}_{hml}$), and market ($\hat{a}_{mkt}$) factor returns, the current account to GDP ratio ($\hat{a}_{caf}$) and the term spread ($\hat{a}_{lsi}$); the house price to income ratio ($\hat{a}_{\Delta hg}$) and the house price to rent ratio ($\hat{a}_{\Delta hpr}$); real gold price returns ($\hat{a}_{mr}$).

Moreover, $PC_{\hat{\mathbf{a}}_1}$ loads with negative weight the *ST* components for the unemployment rate ($\hat{a}_{\Delta u}$), real wages growth ($\hat{a}_{rw}$), excess money growth ($\hat{a}_{em}$), and real money growth; the real overnight ($\hat{a}_{oir}$), short-term ($\hat{a}_{sir}$), and long-term ($\hat{a}_{lir}$) interest rates; the momentum factor ($\hat{a}_{mom}$) and the real effective exchange return ($\hat{a}_{ref}$); the fiscal deficit to GDP ratio ($\hat{a}_{fdg}$), the house price gap ($\hat{a}_{\Delta hg}$) and the credit gap ($\hat{a}_{\Delta cg}$); the implied Stoxx index volatility ($\hat{a}_{vstx}$) and the Euribor-Eonia spread ($\hat{a}_{soi}$); the composite indicator of systemic sovereign stress ($\hat{a}_{sci}$) and the composite financial condition index ($\hat{a}_{ciss}$).

Hence, a typical improvement in the short-term, *cyclical* macro-financial environment in the euro area would be characterized by an increase in cyclical GDP growth and inflation, a countercyclical decrease in real wages, and a contraction in cyclical unemployment. The improvement in cyclical economic conditions is also reflected in the procyclical response of the Fama-French size and value factor returns, as well as in the countercyclical response of momentum.

Moreover, real short and long-term interest rates would contract, as well as nominal excess money growth and real money growth. This pattern implicitly suggests that nominal interest rates would increase less than proportionally during economic upturns relative to inflation changes. This feature is less evident at longer maturities; coherently, the term spread would increase. Yet, liquidity and credit to the private sector would expand less than proportionally than real GDP growth and inflation changes, providing a stabilizing impact.

Moreover, a countercyclical pattern is detected for fiscal policy. The fiscal deficit to GDP ratio would tend to worsen during economic upturns. Differently, the current account would tend to improve, concurrent with a real depreciation of the effective exchange rate.

Short-term, cyclical economic upturns are also phases of rising asset prices, as shown by the stock and house price series, as well as periods of overall financial stability, as shown by decreasing financial condition indexes (*ciss* and *sci*), stock volatility, and interbank rate spreads. Interestingly, gold returns are procyclical, different from what is detected for their medium to long-term dynamics.

Symmetrically, a typical worsening in short-term, cyclical conditions would be characterized by opposite dynamics to those described above.

5. Macro-financial fluctuations in the euro area

In light of their information content, our composite indexes of macro-financial conditions (*MF*) are then based on the first principal components extracted from the sets of *MLT* and *ST* series ($PC_{\hat{\mathbf{n}}_1}$ and $PC_{\hat{\mathbf{a}}_1}$). In particular, $PC_{\hat{\mathbf{n}}_1}$ and $PC_{\hat{\mathbf{a}}_1}$ are re-scaled, to grant to the *MF* indicators the interpretation of *conditional expectation* for the year-on-year monthly GDP growth rate, where conditioning is made to a given macro-financial information set, as subsumed by the estimated principal components themselves.

We then have

$$MFt_t \equiv E\left[\widehat{\in g_t | PC_{\hat{\mathbf{n}}_1,t}}\right] = \hat{\mu}_{\in g} + \hat{\beta}_n PC_{\hat{\mathbf{n}}_1,t}, \tag{15}$$

where $\hat{\mu}_{\in g}$ is the sample mean of the monthly year-on-year €*coin* GDP growth rate ($\in g_t$) and $\hat{\beta}_n = \frac{Cov(\widehat{\in g, PC_{\hat{\mathbf{n}}_1}})}{Var(\widehat{PC_{\hat{\mathbf{n}}_1}})}$. Hence, MFt_t is computed as the fitted component from the OLS regression of $\in g_t$ on a constant term and (the zero mean) $PC_{\hat{\mathbf{n}}_1,t}$. The *MFt* indicator then bears the interpretation of *expected* (year-on-year monthly) *trend GDP growth rate*, given current underlying macro-financial developments. Hence, it provides information on medium to long-term economic developments, stemming from long swings in real activity, the financial cycle, and their interaction.

Similarly, we can compute

$$MFc_t \equiv E\left[\widehat{\in g_t - \hat{\mu}_{\in g} | PC_{\hat{\mathbf{a}}_1,t}}\right] = \hat{\beta}_c PC_{\hat{\mathbf{a}}_1,t}, \tag{16}$$

from the fitted component of the OLS regression of (the demeaned) $\in g_t$ on $PC_{\hat{\mathbf{a}}_1,t}$. The *MFc* indicator then yields the *expected* (year-on-year monthly) *cyclical GDP growth rate*, given current short-term macro-financial developments. It is therefore informative on macro-financial interactions at business cycle frequencies.

Finally, we have

$$MF_t \equiv E\left[\widehat{\in g_t | PC_{\hat{\mathbf{n}}_1,t}}, PC_{\hat{\mathbf{a}}_1,t}\right] = \hat{\mu}_{\in g} + \hat{\beta}_n PC_{\hat{\mathbf{n}}_1,t} + \hat{\beta}_c PC_{\hat{\mathbf{a}}_1,t}, \tag{17}$$

from the fitted component of the OLS regression of $\in g_t$ on a constant term, $PC_{\hat{\mathbf{n}}_1,t}$ and $PC_{\hat{\mathbf{a}}_1,t}$. This yields the *expected* (year-on-year monthly) *overall GDP growth rate*, given current medium to long-term (*trend*) and short-term (*cyclical*) macro-financial developments. Notice that $PC_{\hat{\mathbf{n}}_1,t}$ and $PC_{\hat{\mathbf{a}}_1,t}$ are orthogonal by construction. Hence, the fitted component from the multivariate model in (17) is equivalent to the sum of the univariate estimates obtained from (15) and (16).

Hence, in the light of the above definition, an increase in *MF* (*MFt*, *MFc*) can be associated with an improvement in the macro-financial context and in the pace of GDP growth at the *overall* (*trend*, *cyclical*) level.

The estimated regression in (17) is reported in Table 3, Panel E. As is shown in the Table, about 55% of annualized monthly GDP growth is accounted by (common) macroeconomic and financial interactions; of these, about 20% reflect medium to long-term interactions occurring at financial cycle frequencies, while about 35% reflect short-term interactions occurring at business cycle frequencies.
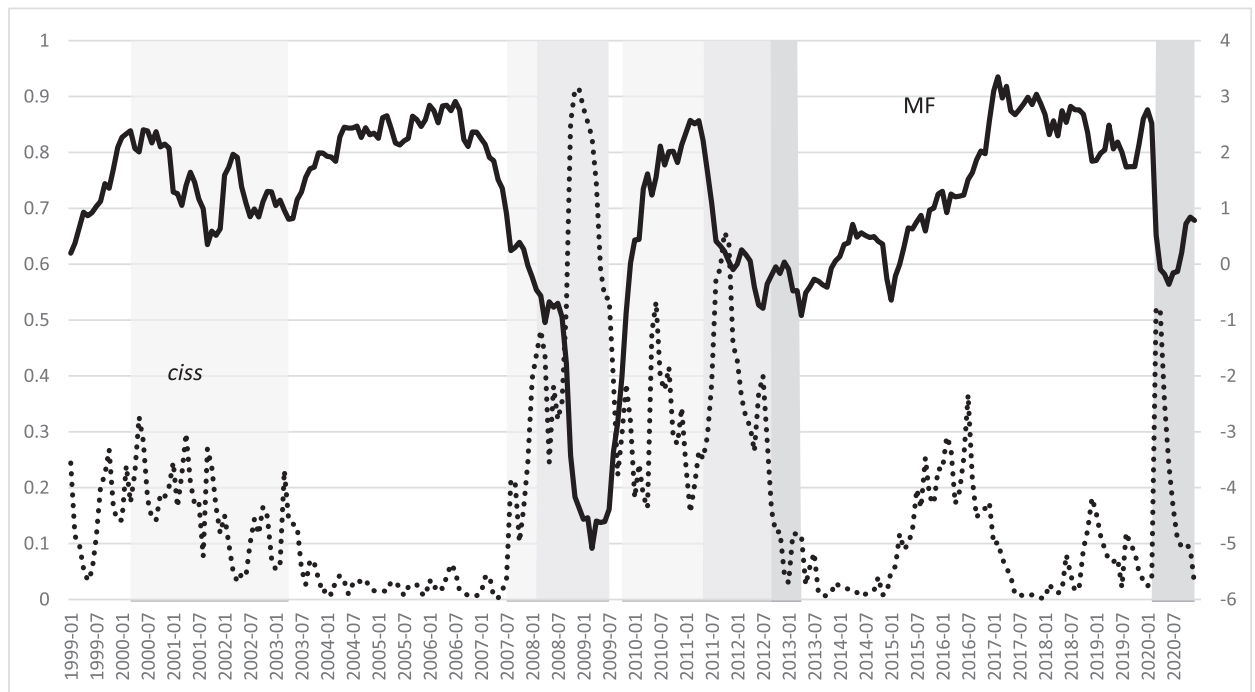
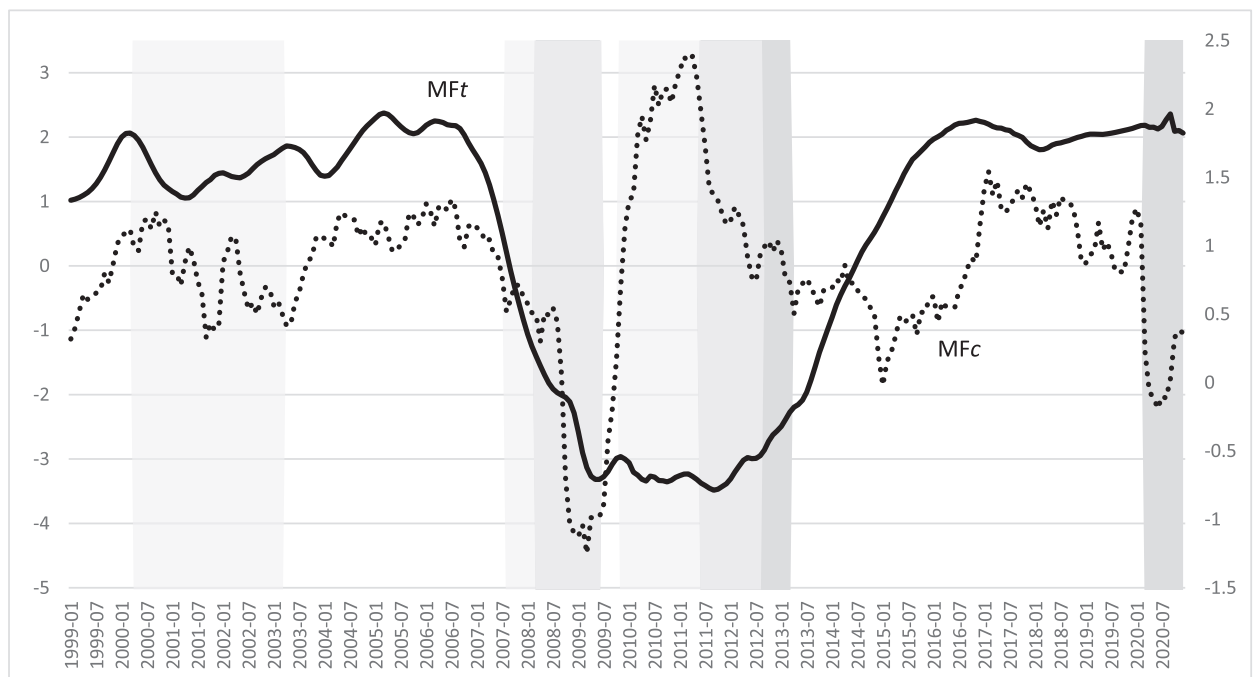**Fig. 3.** macro-financial indicator (MF; rhs) vs. ciss (lhs)

Fig. 4. macro-financial indicator (MF); trend (MFt; rhs) vs. cyclical component (MFc; lhs)

Finally, notice that the use of PCA for the computation of the macro-financial condition indexes can be justified based on its noise suppression properties: intuitively, PCs associated with the smallest eigenvalues measure noise features, which are then neglected when estimating the composite index using the first PC of each set of *MLT* and *ST* components (as in the current case), or their first few PCs, depending on data properties.
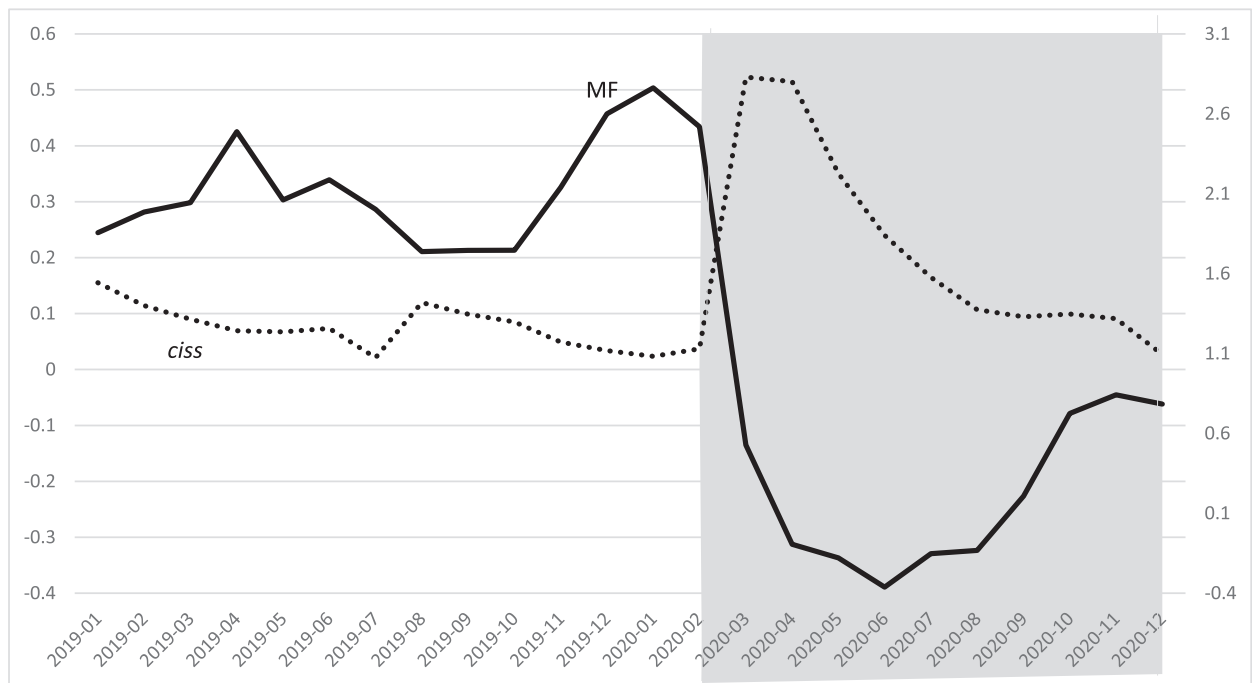
Fig. 5. macro-financial indicator (MF; rhs) vs. ciss (lhs) over the pandemic

In Figures 3-4 the estimated macro-financial indicators (*MF*, *MFt*, and *MFc*) are plotted over the available time span. Moreover, in Figures 5-6 the same indicators are plotted over the period 2019:1 through 2020:12, to zoom over the pre-pandemic and pandemic periods, and better gauge their information content over the pandemic crisis.

In Figures 3 and 5, the *ciss* indicator is also plotted, to contrast the information content of the two indicators. Since *ciss* is one of the components of the *MF* indicator, the comparison should be informative about the potentially higher informational content of *MF* relative to *ciss*. In this respect, notice that while an increase in *MF* (*MFt*, and *MFc*) is associated with an improvement in macro-financial conditions, an increase in *ciss* is associated with worsening conditions. We, therefore, expect *MF* and *ciss* to be negatively correlated.

As shown in Figures 3 and B3a (Online Appendix), the *MFt* component provides, as expected, valuable information on the financial cycle. According to the evidence, almost two complete boom-bust phases appear to characterize the euro area financial cycle. In terms of peak-to-peak chronology, we mark the first financial cycle peak in May 2006. The bust phase in the financial cycle then appears to lead the financial crisis of about fifteen months. Its trough spans over about two years, between the end of the Great Recession and the early phase of the sovereign debt recession (June 2009-October 2011). At this stage, it is still uncertain whether the pandemic has marked the peak of the second financial cycle, due to the resilience of the underlying macro-financial context during the current recession.

In the plots, we also include details about the timing of the various economic and financial distress episodes that occurred since the early 2000s. According to EABCN chronology, over the period investigated there have been two complete cyclical episodes (recession followed by expansion), i.e. 2008 Q1 (Peak) through 2009 Q2 (Trough), 2011 Q3 (Peak) through 2013 Q1 (Trough). These recession episodes then span March 2008 through June 2009 (included) and June 2011 through March 2013 (included). A new recession episode, associated with the COVID-19 pandemic, has occurred since 2020 Q1, most likely since March 2020, continuing throughout the end of our sample, i.e. December 2020.

On the other hand, the financial episodes timeline is as follows. Concerning the dot-com bubble: April 2000 (start) and March 2003 (end), where we associate the beginning of the crisis with the burst of the stock market bubble, i.e. the beginning of the persistent decline in the S&P500 index, which lasted through February 2003; the end of the bust is then marked by the steady stock market recovery beginning in March 2003. For the subprime financial crises: August 2007 (start) and June 2009 (end), where we associate the beginning of the crisis with BNP-Paribas announcing its inability to price three of its investment funds based on US subprime mortgage loans and its end with the *normalization* of the short-end of the LIBOR-OIS swap rates term structure (i.e., with the normalization in interbank market conditions). Within this period also commodity and stock markets were heavily destabilized. See Cassola and Morana (2012) and Morana (2014c) for supporting empirical evidence. Concerning the EA sovereign debt crisis, we mark the beginning of the crisis with the Greek prime minister George Papandreou's revealing that Greek public finances were far worse than previous announcements, with a year deficit of 12.7% of GDP and a public debt of $410 billion, in October 2009. On the other hand, we mark the end of the crisis between March and August 2012, following the implementation of the second bailout package for Greece in February
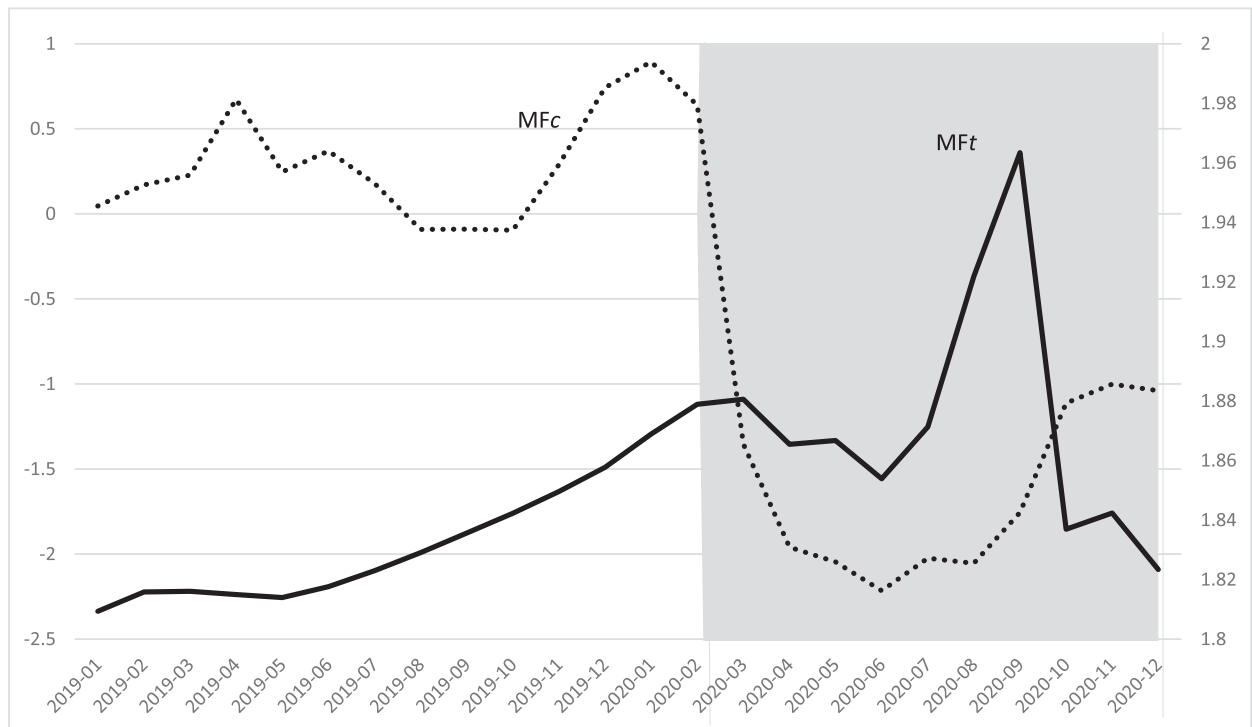
Fig. 6. macro-financial indicator (MF); trend (MFt; rhs) vs. cycle (MFc; lhs) over the pandemic

2012 (with private holders of Greek government bonds accepting a slightly bigger haircut than expected), EU member states agreeing to an additional retroactive lowering of the bailout interest rates, and the ECB held its second long term refinancing operation, which provided EA banks with further € 529.5 billion in loans. This led to a persistent normalization of the EA interbank market since March 2012, which, under stress again since early 2010, was fully accomplished by August 2012. It could, however, be argued that the euro area crisis came to the end only in 2015, as the ECB started its Quantitative Easing Policy, and a new, third bailout program for Greece was enacted by the European Commission, the ECB, and the IMF. Indeed economic growth was restored in *all* Eurozone countries only in 2016.

5.1. The pre-pandemic macro-financial environment

As shown in Figures 3-4, the interpretation of *MF* and its components, *MFt* and *MFc*, in terms of macro-financial indicators is supported by the graphical evidence. For instance, evidence of deteriorating macro-financial conditions can be noted in association with the early 2000s stock market crisis. This deterioration appears to have initially concerned both trend and cyclical conditions. Expected annual trend GDP growth contracts -0.4%, from 1.8% to 1.4% (peak to trough over the period 2000:3 to 2001:5). Moreover, expected cyclical GDP growth contracts -1.7%, from 0.6% to -1.1% (2000:3 to 2001:9). As cyclical conditions dominate trend conditions, expected overall GDP growth contracts -2% from 2.4% in 2000:3 to 0.4% in 2001:9. It then rises to 0.8% in 2003:4, as the recovery in the underlying macro-financial context partially compensates persisting weakness in cyclical conditions.

Early warnings of incoming macro-financial stress are then conveyed by *MF* for the late 2000s financial crisis, as well as at the beginning of the euro area sovereign debt crisis. *MF* persistently declines over the period 2006:7 through 2009:3, therefore anticipating the subprime financial crisis, started in August 2007, of about one year. This signal appears to be conveyed by both the trend and cyclical components of the indicator. The deterioration of growth prospects during the Great Recession was most sizable in terms of expected cyclical GDP downturn, as *MFc* contracts -5.7%, from 1% to -4.7% (peak to trough over the period 2006:7 to 2009:3); the contraction in expected trend GDP growth is however also very sizable, i.e. -2.6%, from 1.9% to -0.7% (2006:7 to 2009:6). Coherently, the contraction in expected overall GDP growth is -7.9%, from 2.9% to -5% (2006:7 to 2009:3).

As shown in Figure 4, macro-financial improvements during the recovery period from the Great Recession (2009:7 through 2011:4) concern cyclical conditions only, while a persistent stagnation can be noted for trend conditions (-0.7% on average annually). Hence, the sovereign debt crisis appears to have contributed to delay the recovery in trend GDP growth in the euro area. Deteriorating macro-financial conditions are detected again over the period 2009:10 through 2011:10 by *MFt*, consistent with the beginning of the euro area crisis. The crisis then reached a sizable, euro area dimension only much

later, i.e. when contagion eventually affected Italy in summer 2011. Even concerning Greece alone, the first bailout package was not implemented any earlier than in May 2010. Hence, MFt not only shows some leading indicator properties for the euro area sovereign debt crisis, but it also provides a consistent accounting of its development.

A further deterioration in macro-financial conditions is then signaled by MF during the sovereign debt recession, followed by a persistent improvement in the post-recession period; recovery peaks at 2017:2. By comparing pre-crisis and post-crisis conditions, it can be concluded that it took about a decade to return to pre-crisis overall macro-financial conditions and expected growth pace, estimated at an annual GDP growth rate of about 3.4% by MF. As shown in Figure 4, this recovery was mostly driven by trend macro-financial conditions (MFt) initially. As shown by MFc, the recovery in cyclical macro-financial conditions only started in 2015:2, i.e. following the inception of the Q.E. monetary policy in 2015:1. Cyclical recovery then appears to have accelerated over the most expansionary phase of Q.E. (2016:4-2017:3).

A progressive worsening in overall macro-financial conditions is signaled by MF since 2017:3, concurrent with the phasing out of the Q.E. policy (completed in 2018:12), lasting throughout 2019. Yet as shown in Figure 5, most of this worsening concerns cyclical macro-financial conditions. The underlying macro-financial context, as measured by MFt, appears to have only temporarily worsened: expected trend GDP growth initially falls from its 1.9% peak annual rate in 2017:2 to 1.7% in 2018:3. It then reverts to 1.9% in 2020:2. On the other hand, the worsening in cyclical macro-financial conditions since 2017:3 is persistent, as the expected cyclical GDP growth rate falls from a 1.5% annual rate in 2017:2 down to 0.9% in 2020:2.

For comparison, in Fig. 3 we also report the composite indicator of systemic stress ($ciss$). The comparison of developments in $ciss$, MF, and its components MFt and MFc, over time, confirms the expected negative correlation for these indicators; yet, the additional macro-financial information contained in MF appears to be sizable, since the estimated correlation coefficients for the pairs $ciss - MF$, $ciss - MFt$, $ciss - MFc$, are only about -0.7, -0.6. and -0.4, respectively. In terms of early warning signals, apart from the early 2000s bust episode, the $ciss$ indicator appears to show coincident, rather than leading indicator properties, well marking the timing of the various episodes of financial and economic stress that occurred in the sample, rather than providing anticipatory signals.

5.2. The pandemic macro-financial environment

As shown in Figure 6, the pandemic does not appear to have sizably affected trend macro-financial conditions so far. In this respect, the expected trend GDP growth rate (MFt) has only moderately declined (-0.1%), contracting to an annual rate of about 1.8%. On the other hand, the impact on cyclical macro-financial conditions (MFc) has been very deep. The expected cyclical GDP growth rate has first fallen to a -2.2% annual rate over the period 2020:4 through 2020:8; since 2020:9 a small recovery in expected cyclical GDP growth can be noted, up to a -1% annual rate. By considering the contribution of the trend and cyclical components, weak overall expected GDP growth (MF) is then pointed out (0.8%). Differently, as shown in Figure 5, the $ciss$ indicator points to a prompt and sizable increase in financial stress in 2020:3-4; then to its progressive resolution since 2020:5. Hence, according to $ciss$, stress-free financial conditions appear to hold over the second semester of the year 2020. Yet the pandemic is not over, the economic contraction is still large, the expected recovery uneven across countries and sectors, and the risk of new episodes of financial stress, as arising from both corporate and sovereign debt, palpable (European Council (2021)). The lack of any signals from $ciss$ is somewhat at odds with the perceived features of the current macro-financial context.

Overall, the resilience of the underlying macro-financial context in the euro area is consistent with the prompt expansionary monetary and fiscal policy mix implemented by the European Commission and the European Central Bank since the inception of the pandemic crisis. In this respect, a new Q.E. monetary policy was started in March 2020 by the ECB, i.e. the pandemic emergency purchase program (PEPP), consisting of monthly net asset purchases of € 120 billion through the end of 2020. Since then, the ECB has further increased the PEPP by € 500 billion to a total of € 1,850 billion in December 2020, and extended it at last throughout March 2022. A small upward jump in expected trend GDP growth can be even noted over summer 2020, as the "Next Generation EU" recovery plan, proposed in May-June 2020, was eventually finalized in July 2020 and approved in November 2020. The agreement integrates the 2021-27 EU long-term budget (MFF 2021-2027) of € 1074,3 billion with the temporary instrument for recovery "Next Generation EU" of € 750 billion.

5.2.1. Policy implications

As shown in Figures 3-4, the pre-pandemic period can be described as a period of stable trend growth, at levels consistent with pre-financial crisis conditions, and where the financial cycle might have reached a peak area. Some decline in cyclical growth can however be noted. This slowing down in cyclical growth might be possibly related to the exit from the Q.E. policy in December 2018. Since then, cyclical macro-financial conditions appear to have stagnated up to November 2019, when net asset purchases restarted at a monthly pace of € 20 billion. Following this new expansionary monetary policy intervention, expected cyclical GDP growth surged to a 0.5% annual rate.

Hence, the Q.E. monetary policy appears to have exercised a most important role in restoring cyclical growth in the euro area since 2015. Our estimates suggest that, over its most expansionary phase, the expected cyclical GDP growth rate rose to a 1% annual rate. In the light of this evidence, it is likely that the pandemic emergency purchase program (PEPP), started in March 2020, might have contributed to contain the contraction in cyclical GDP growth, as well as to the resilience of trend GDP growth.

But the pandemic is far from being over and the risk for a further worsening in the economic environment high, particularly concerning sovereign and corporate debts (Ehnts and Paetz, 2021). In this respect, our evidence shows that the euro area sovereign debt crisis and associated recession delayed trend GDP growth recovery from the Great Recession and slowed down cyclical GDP growth in the post-crisis period. A new phase of sovereign debt instability and austerity policies, within the current pandemic context, would likely exercise similar effects. It is therefore mandatory, that the Q.E. policy be continued until recession impulses are fully exhausted, to grant liquidity to the banking, corporate and public sectors.

The implementation of the largest stimulus package ever financed through the EU budget in December 2020, coupled with "Next Generation EU", is surely an important discontinuity relative to the austerity policies recommended to contain public deficits during the sovereign debt crisis. The package has made available a total of about € 1.8 trillion to fight against the pandemic, sustain recovery in Europe, and start the *green transition* towards a carbon-free economy by 2050. This transition, to be accomplished, will require massive public and private investment in the research and innovation sectors, digital technologies, health and medical programs, sustainable agriculture and animal farming, green energy production, sustainable transportation. In so far as the green transition, as the fight against the pandemic, is an "objective of the EC", it is on the EC, not on the EU single member states, to generate the resources to achieve this objective. The fight against the pandemic has started an unprecedented course of action for the EC, which is also the first step in the implementation of the EU Green Deal strategy. The achievement of its long-term objective of carbon neutrality does appear to require that the EC will keep issuing European sovereign bonds to allocate grants and loans to its member states, with the objective of funding not only the fight against the pandemic, but also the green "modernization" of the EU economy. This long wave in private and public investments will have, as a by-product, the additional benefit of mitigating the euro area saving glut, which, as measured by the underlying current account surplus to GDP ratio, has been steadily growing since the sovereign debt crisis (Figure B2a in the Online Appendix).

As the pandemic is ongoing, the continuation of the EC-ECB expansionary fiscal and monetary policy mix is also suggested to prevent a new major financial crisis, which, very likely, would trigger the bust phase of the financial cycle. Based on our empirical evidence, a typical medium to long-term macro-financial downturn is characterized by falling stock and house prices, interbank and sovereign debt market stress and a persistent contraction in credit flows to the private sector. These mechanics would surely be magnified in the already highly leveraged euro area financial environment. In fact, according to OCED estimates, the leverage ratio for the financial sector in 2019 was over or about 20% for France, Germany, and Italy (and Luxembourg); about 15% for the Netherlands, Spain, Greece, and the Slovak Republic (not reported). The current risk of financial disruptions is therefore high.

As shown by the Great Recession episode, major financial crises can impact GDP growth in the medium to long term; the contraction might not only be deep, but also very persistent. Given the already low and declining current level of inflation (see Figure B1c in the Online Appendix), a joint worsening in short- and medium to long-term macro-financial conditions would then likely trigger a sizable and persistent deflation. The emergence of a *deflation trap* is the ultimate worst-case scenario we envisage, in so far as the policy response to the pandemic crisis did not prevent a financial bust eventually.

5.3. Predictive ability of the macro-financial indicators

In this section we focus on the out-of-sample forecasting power of the proposed indicators, in terms of their forward-looking properties for GDP growth developments. These are measured by the *p*-lead one-side moving average of the annualized monthly GDP growth rate, with $p = 1, ..., 24$. Hence, the exercise aims to assess the ability of the indicators to signal GDP growth changes at both high and low frequencies, i.e. at both the cycle and trend levels.

The predictive OLS regression is

$$y_{t+1}^* = \alpha_{p,t} + \beta_{p,t} x_t + \varepsilon_{p,t}, \tag{18}$$

where $y_{t+1}^* = \frac{1}{h} \sum_{h=1}^p y_{t+h}$, $p = 1, ..., 24$, y_t is the annualized €-coin index, and $x_t = \widehat{MFt}_{t|t}$, $\widehat{MFc}_{t|t}$, $ciss_t$, $t = T^*, ..., T - p$, where we set $T^* = 265$, in order for the out of sample forecasting exercise to span over up to the last 100 observations in the sample, using the initial 165 observations for the initial "training" of the model. Estimation of the model is however implemented recursively and therefore allows for parameters updating.

Moreover, we also consider the following predictive OLS regression

$$y_{t+1}^* = \alpha_{p,t} + \beta_{t,t} \widehat{MFt}_{t|t} + \beta_{c,t} \widehat{MFc}_{t|t} + \varepsilon_{p,t}, \tag{19}$$

in order to asses the predictive power of both *MF* components jointly.

Hence, in the exercise, we compare the 1-step ahead out of sample forecasting ability of the *feasible* trend ($\widehat{MFt}_{t|t}$) and cyclical ($\widehat{MFc}_{t|t}$) components of the *MF* indicator and the *ciss* indicator.

The results of the forecasting exercise are reported in Figure 7, where we plot the RMSFE for $\widehat{MFt}$, $\widehat{MFc}$ and both components jointly considered ($\widehat{MFu}$), relative to the RMSFE for the *ciss* indicator ($RMSFE_i/RMSFE_{ciss}$; $i = MFt$, MFc, MFu). Hence, values smaller than unity in the plot indicate overperformance of the *MF* indicators relative to the *ciss* indicator.

As shown in the plot, the results of the forecasting exercise are clear-cut, pointing to excess forecasting power of the *MF* and its components over *ciss* at most aggregation levels. The *MFt* component overperforms any of the other indicators
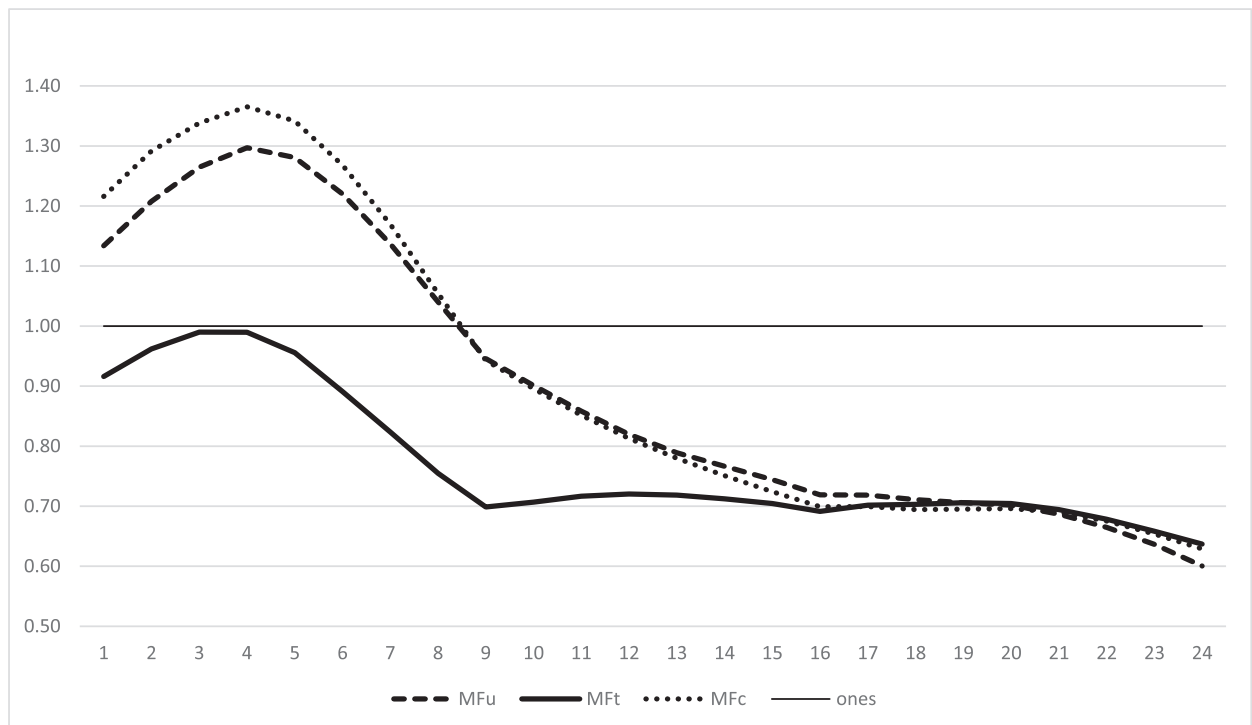
Fig. 7. Out of sample forecasts: RMSFE relative to ciss

at any aggregation interval, with forecasting overperformance being highest from $p = 9$ and larger aggregation intervals. The RMSFE improvement at these intervals is very sizable, i.e. about 30%. This is consistent with the fact that MF_t is indeed devised to have predictive power for the *underlying* evolution of GDP growth, and therefore not responsive to erratic changes in the series. Since the *ciss* indicator is a component of the *MF* indicator, the congruency of the signals provided by the two indicators at some aggregation intervals is not surprising. Yet, by exploiting additional macroeconomic and financial information, *MF* appears to show stronger leading indicator properties, which make it suitable for use within an early warning system of macro-financial indicators.

6. Conclusions

In this paper, we introduce a new time-domain decomposition for weakly stationary or trend stationary processes, based on trigonometric polynomial modeling of the underlying component of an economic time series. The method is explicitly devised to disentangle medium to long-term and short-term fluctuations in macroeconomic and financial series, to allow for an accurate assessment of the financial cycle and the concurrent long swings in economic activity. Financial cycles appear to be concurrent with medium-term economic fluctuations, with a typical periodicity of fifteen to twenty years, lasting therefore much longer than standard business cycle episodes, whose duration, historically, has not exceeded eight years in most countries (Borio, 2014; Borio and Drehmann, 2019).

The implementation of the decomposition is straightforward and relies on standard regression analysis and general to specific model reduction. Full support to the proposed method is provided by Monte Carlo simulation. In the paper, we also provide a multivariate extension for our decomposition, relying on a two-step approach. In the first step, the univariate decomposition is sequentially applied to the set of series of interest. In the second step, the *common* medium to long-term and short-term components are estimated through Principal Components Analysis.

Based on this multivariate approach, we introduce a set of new composite indexes of macro-financial conditions for the euro area. These indexes are devised in such a way to bear the interpretation of expected *overall*, *trend*, and *cyclical* GDP growth. We then use our macro-financial indicators to assess macro-financial conditions in the euro area since its inception. The sample is interesting, as it comprises the early 2000s stock market bubble burst, the 2007-2008 subprime financial crisis and ensuing Great Recession, the sovereign debt crisis, and associated recession, and the current pandemic recession. We find that the proposed indicators provide valuable insights on all the episodes, also showing out-of-sample forecasting power.

In particular, concerning the current pandemic recession, the indicators suggest that most of the GDP contraction has been of short-term, cyclical nature. We think that this is due to the prompt fiscal and monetary policy responses, which not

only have sustained both the supply and demand sides of the euro area economy but have also avoided a major financial crisis.

In this respect, it is still uncertain whether the financial cycle might have currently reached a peak area. As the pandemic is ongoing, the continuation of the expansionary policy mix is then also suggested to prevent a new sovereign/corporate debt crisis, which, otherwise, would likely start the bust phase of the financial cycle. As also shown during the Great Recession, financial crises can exercise sizable and persistent negative effects on medium to long-term GDP growth. Given the already low and declining inflation, a new major financial crisis would be likely coupled with a sizable and persistent deflation. The emergence of a *deflation trap* is the ultimate worst-case scenario we envisage, in so far as the policy response to the pandemic crisis did not prevent the bust phase of the financial cycle.

Acknowledgements

References

Garcia-de Andoain, C., Kremer, M., 2018. Beyond spreads: measuring sovereign market stress in the euro area. ECB Working Paper Series No. 2185.

Bagliano, F.C., Morana, C., 2017. It ain't over till it's over: A global perspective on the great moderation great recession interconnection. Applied Economics 49, 4946–4969.

Bai, J., 2003. Inferential theory for factor models of large dimensions. Econometrica 71, 135–171.

Bai, J., 2004. Estimating cross-section common stochastic trends in nonstationary panel data. Journal of Econometrics 122, 137–138.

Baillie, R.T., Morana, C., 2009. Modeling long memory and structural breaks in conditional variances: An adaptive FIGARCH approach. Journal of Economic Dynamics and Control 33, 1577–1592.

Baillie, R.T., Morana, C., 2012. Adaptive ARFIMA models with applications to inflation. Economic Modelling 29, 2451–2459.

Baxter, M., King, R.G., 1999. Measuring business cycles: approximate band-pass filters for economic time series. Review of Economics and Statistics 8, 575–593.

Beaudry, P., Galizia, D., Portier, F., 2020. Putting the cycle back into business cycle analysis. American Economic Review 110, 1–47.

Beaudry, P., Portier, F., 2014. News-driven business cycles: insights and challenges. Journal of Economic Literature 52, 993–1074.

Becker, R., Enders, W., Lee, J., 2006. A stationarity test in the presence of an unknown number of smooth breaks. Journal of Time Series Analysis 27, 381–409.

Beltratti, A., Morana, C., 2006. Macroeconomic causes of stock market volatility. Journal of Econometrics 131 (8), 151–177.

Bernanke, B. (2005). The global saving glut and the u.s. Current Account Deficit. Speech available at https://www.federalreserve.gov/boarddocs/speeches/2005/200503102/.

Beveridge, S., Nelson, C.R., 1981. A new approach to decomposition of economic time series into permanent and transitory components with particular attention to measurement of the 'business cycle'. Journal of Monetary Economics 7, 151–174.

de Boor, C., 1978. A Practical Guide to Splines. Springer-Verlag, New York.

Borio, C., 2014. The financial cycle and macroeconomics: what have we learnt? Journal of Banking and Finance 45, 182–198.

Borio, C., Drehmann, M.X., 2019. Predicting recessions: financial cycle versus term spread. In: BIS working papers no. 818.

Borio, C., Lowe, P., 2004. Securing sustainable price stability: should credit come back from the wilderness? In: BIS working papers, no. 157.

Carhart, M.M., 1997. On persistence in mutual fund performance. The Journal of Finance 52, 57–82.

Cassola, N., Morana, C., 2012. Euro money market spreads during the 2007-? financial crisis. Journal of Empirical Finance 19, 548–557.

Castle, J.L., Doornik, J.A., Hendry, D.F., 2021. Robust discovery of regression models. Econometrics and Statistics doi:10.1016/j.ecosta.2021.05.004. Forthcoming. Available at

Christiansen, C., Eriksen, J.N., Møller, S.V., 2019. Negative house price co-movements and US recessions. Regional Science and Urban Economics 77, 382–394.

Cipollini, F., Gallo, G.M., 2019. Modeling euro STOXX 50 volatility with common and market-specific components. Econometrics and Statistics 11, 22–42.

Clark, P.K., 1987. The cyclical component of us economic activity. Quarterly Journal of Economics 102, 797–814.

Dittmann, I., Granger, C.W.J., 2002. Properties of nonlinear transformations of fractionally integrated processes. Journal of Econometrics 110, 113–133.

Doornik, J.A., 2009. Autometrics. In: Castle, J.L., Shephard, N. (Eds.), The methodology and practice of econometrics: Festschrift in honour of david f. hendry. Oxford University Press, Oxford.

Ehnts, D., Paetz, M., 2021. COVID-19 and its economic consequences for the euro area. Eurasian Economic Review doi:10.1007/s40822-020-00159-w.

Engle, R.F., Kozicki, S., 1993. Testing for common features. Journal of Business & Economic Statistics 11, 369–379.

Ermini, L., Granger, C.W.J., 1993. Some generalizations on the algebra of i(1) processes. Journal of Econometrics 59, 369–384.

European Council (2021). Eurogroup statement on the euro area fiscal policy response to the COVID-19 crisis and the path forward. Available at https://www.consilium.europa.eu/en/press/press-releases/2021/03/15/eurogroup-statement-on-the-euro-area-fiscal-policy-response-to-the-covid-19-crisis-and-the-path-forward/.

Fama, E.F., French, K.R., 1993. Common risk factors in the returns on stocks and bonds. Journal of Financial Econonomics 33, 3–56.

Gallant, A.R., 1981. On the bias in flexible functional forms and an essentially unbiased form: the fourier flexible form. Journal of Econometrics 15, 211–245.

Gallant, A.R., 1984. The fourier flexible form. American Journal of Agricultural Economics 66, 204–208.

Granger, C.W.J., Hallman, J., 1991. Nonlinear transformations of integrated time-series. Journal of Time Series Analysis 12, 207–224.

Guender, A., 2018. Credit prices vs credit quantities as predictors of economic activity in europe: which tell a better story? Journal of Macroeconomics 57, 380–399.

Hamilton, J.D., 1994. Time Series Analysis. Princeton University Press.

Hamilton, J.D., 2018. Why you should never use the hodrick-prescott filter. Review of Economics and Statistics 100, 831–843.

Harvey, A.C., 1985. Trends and cycles in macroeconomic time series. Journal of Business & Economic Statistics 3, 216–227.

Harvey, A.C., Jaeger, A., 1993. Detrending, stylized facts and the business cycle. Journal of Applied Econometrics 8, 231–247.

Hendry, D.F., 1995. Dynamic Econometrics. Oxford University Press, Oxford.

Hendry, D.F., Johansen, S., Santos, C., 2008. Automatic selection of indicators in a fully saturated regression. Computational Statistics 33, 317–335. Erratum. 337-339

Hodrick, R.J., Prescott, E.C., 1997. Postwar US business cycles: an empirical investigation. Journal of Money, Credit, and Banking 29, 1–16.

Hollo, D., Kremer, M., Lo Duca, M., 2012. CISS - a composite indicator of systemic stress in the financial system. ECB Working Paper No. 1426.

Jordà, O., Schularick, M., Taylor, A.M., 2013. When credit bites back. Journal of Money Credit and Banking 45, 3–28.

Kapetanios, G., Price, S., Young, G., 2018. A UK financial conditions index using targeted data reduction: Forecasting and structural identification. Econometrics and Statistics 7, 1–17.

Lee, J., Enders, W., 2012. The flexible fourier form and the dickey-fuller type unit root tests. Economics Letters 117, 196–199.

Levine, R., 2005. Finance and growth: Theory and evidence. In: Aghion, P., Durlauf, S.N. (Eds.), Handbook of economic growth. Elsevier, Amsterdam. 865-934

Liu, W., Mönch, E., 2016. What predicts US recessions? International Journal of Forecasting 32, 1138–1150.

Morana, C., 2007. Multivariate modelling of long memory processes with common components. Computational Statistics and Data Analysis 52, 919–934.

Morana, C., 2014a. Factor vector autoregressive estimation of heteroskedastic persistent and nonpersistent processes subject to structural breaks. Open Journal of Statistics 4, 292–312.

Morana, C., 2014b. Insights on the global macro-finance interface: structural sources of risk factor fluctuations and the cross-section of expected stock returns. Journal of Empirical Finance 29, 64–79.

Morana, C., 2014c. New insights on the US OIS spreads term structure during the recent financial turmoil. Applied Financial Economics 24, 291–317.

Morana, C., 2017. The US$/€ exchange rate: structural modeling and forecasting during the recent financial crises. Journal of Forecasting 36, 919–935.

Morana, C., Sbrana, G., 2019. Climate change implications for the catastrophe bonds market: an empirical analysis. Economic Modelling 81, 274–294.

Nelson, C.R., Plosser, C.R., 1982. Trends and random walks in macroeconmic time series: some evidence and implications. Journal of Monetary Economics 10, 139–162.

Phillips, P.C.B., Shi, Z., 2020. Boosting: why you can use the HP filter. International Economic Reiew doi:10.1111/iere.12495.

Ponka, H., 2017. The role of credit in predicting US recessions. Journal of Forecasting 36, 469–482.

Ravn, M., Uhlig, H., 2002. On adjusting the hodrick–prescott filter for the frequency of observations. The Review of Economics and Statistics 84, 371–376.

Schwert, .W., 1989a. Business cycles, financial crises, and stock volatility. Carnegie-Rochester Conference Series on Public Policy 31, 83–125.

Schwert, .W., 1989b. Why does stock market volatility change over time? The Journal of Finance 44, 1115–1153.

Watson, M.W., 1986. Univariate detrending methods with stochastic trends. Journal of Monetary Economics 18, 49–75.